ANALYSIS, DESIGN, AND EVALUATION OF THE OPTIMUM TOPOLOGY CUK CONVERTER IN COMPARISON WITH THE CONVENTIONAL BUCK-BOOST CONVERTER

by

Ching Jang Wu

Dissertation submitted to the Faculty of the
Virginia Polytechnic Institute and State University
in partial fulfillment of the requirements for the degree of
DOCTOR OF PHILOSOPHY
in
Electrical Engineering

APPROVED:

T. W. Nehl, Chairman

N. A. Demerdash

F. A. Fouad

L. W. Johnson

R. H. Miller

October, 1981

Blacksburg, Virginia

ACKNOWLEDGEMENTS

The author wishes to express his deepest gratitude to Dr. T. W. Nehl, Chairman of my committee, whose continued support, encouragement and advice throughout the course of this research have made this work possible. His guidance as adviser and friend is heartily acknowledged.

In addition, the author would like to express his sincere appreciation to the members of his graduate committee--Dr. N. A. Demerdash, Dr. F. A. Fouad, Dr. L. W. Johnson, and Dr. R. H. Miller for their valuable suggestions and comments which have resulted in a more complete document.

Also, the author acknowledges the excellent typing of in preparing the final form of this dissertation.

Thanks are extended to for proofreading and suggestions on the use of the English language.

Finally, the author wishes to express sincere appreciation to his parents for their encouragement and support which have provided the strength and drive for the successful completion of this work.

TABLE OF CONTENTS

CHAPTER 1

INTRODUCTION

The series-pass regulator, using the transistor as a nonlinear variable resistor, was the most frequently used power supply before the switched-mode power converters became popular. Due to the low operating efficiency and the bulky filters, these conventional power supplies (1-4) have been replaced by the switched-mode power converters in the last decade. Recently, the trend has been to operate the switched-mode power converters at as high a frequency as possible (5-10). The motivation for going to higher frequency operation is the constant pressure from aerospace and commercial applications for smaller sizes and lower weights. Of course, a less appreciated benefit of higher frequency operation is the increased control loop bandwidth that results in a faster transient response. Because of their lower internal losses, smaller size, lower weight and costs compared to the conventional series-pass or linear power supplies, the switched-mode regulators are in the process of revolutionizing the power supply industry. However, the advantages offered by switched-mode power converters are only possible if the following two important factors are accounted for during the design process:

1. Early in the design process, a decision must be made on the switching frequency. The choice of switching frequency is complicated by the fact that most design parameters (weight, size and efficiency, etc.) change rather slowly with increasing frequency. There

is relatively little advantage to be gained by increasing the switching frequency by a factor of two or three. The switching frequency must be increased high enough to make the reduction of magnetic and capacitive components well worthwhile because of the fact that the switching and magnetic losses increase rapidly at higher frequencies.

The choice of switching frequency is complicated by other factors such as the power converter specifications, the choice of power switches (bipolar or power MOSFET), and the power level, etc. Selecting a switching frequency based purely on a designer's experiences, results in, in most cases, a piecemeal suboptimum design.

(2) The most attractive advantage of operating a switching converter at a higher frequency range (with the present technology, transistors can be operated to the hundred KHZ range, power MOSFET to the MHZ range) is the reduction in volume of the magnetic components, such as, transformers, inductors, and capacitors. Because of the reduction of core cross sectional area, wire size and the number of turns at higher frequencies, improper selection of the magnetic components often result in cores with too much window area. As a result, the proportions of the core design are often not optimum. Though the magnetic sizes decrease with higher switching frequency, improper design of magnetic components could increase the weight penalty due to the increased magnetic losses.

This dissertation presents a detailed analysis and comparison of two of the most popular and functionally similar switching power converters, that is, the conventional Buck-Boost converter and the Cuk converter as shown in Figure (1.0-1). Detailed comparisons and

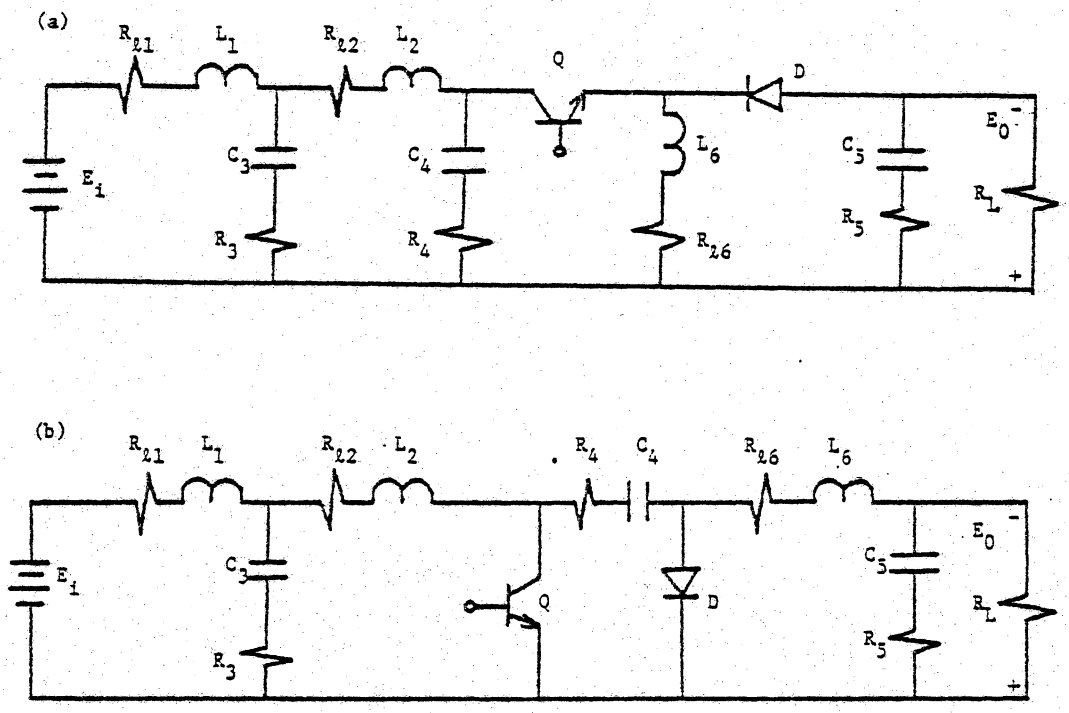

Figure (1.0-1) Circuit Diagrams

(a) Buck-Boost Converter

(b) Cuk Converter

evaluations are made of these two converters in light of total circuit weight and power losses. A powerful and efficient nonlinear programming technique using the penalty function method is employed for the comparisons. In the comparison process, the two important factors related to switching power converter design as posed above are solved. Both the Buck-Boost converter and the Cuk converter perform the same function of either stepping up or stepping down the input voltage. The major difference is that the Buck-Boost converter employs the inductor as the energy transfer device and the Cuk converter uses the capacitor for the same purpose. Before presenting the detailed comparison of the two converters, the motivation behind the research work is briefly described in the following.

1.1 Motivation of the Research Work

(1) Motivation for the comparison of these two converters

The comparison of these two converters is motivated by research conducted by Landsman and Wood (11,12) and a series of publications (13-22) by Middlebrook and Cuk. In 1977, Cuk disclosed, for the first time, the new optimum topology Cuk converter which is characterized by nonpulsating input and output currents. The existing Buck-Boost converter, as shown in Figure (1.1-1a), combines the undesirable pulsating input current of the Buck converter and the undesirable pulsating output current of the Boost converter. Instead of cascading the Buck converter by the Boost converter, Cuk cascaded the Boost converter by the Buck converter. This, together with some network manipulation (13), results in the Cuk converter as shown in Figure (1.1-1b).

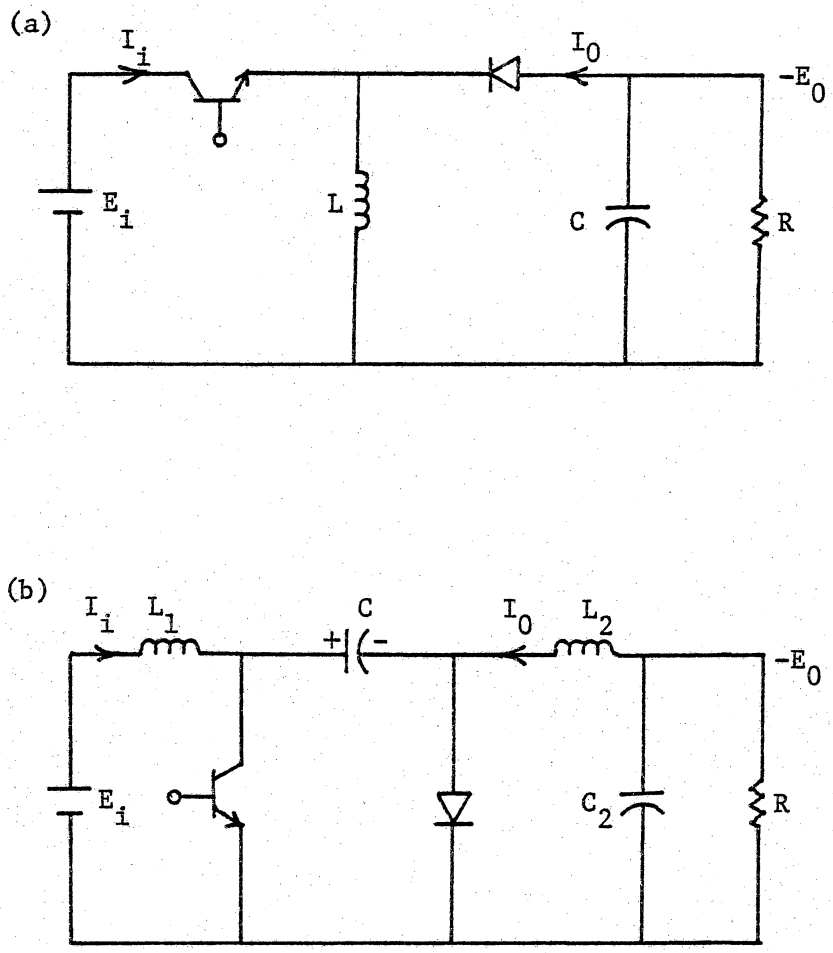

Figure (1.1-1) (a) Basic Buck-Boost Converter

(b) Basic Boost-Buck or Cuk Converter

This Cuk converter preserves the desirable nonpulsating input current of the Boost converter and the nonpulsating output current of the Buck converter. At the same time it performs the function of a conventional Buck-Boost converter of either stepping up or stepping down the input voltage based on the value of the switching duty cycle ratio.

Cuk has claimed that the Cuk converter is the only dc-to-dc converter missing from the existing basic switching converters (i.e., Buck, Boost and Buck-Boost converters). Furthermore, he has claimed that the new converter has all of the advantages and none of the disadvantages of the existing basic converters, such as, smaller switching ripple, higher efficiency, smaller size and weight (13).

In 1979, Landsman derived the Cuk converter and the continuous Buck-Boost converter from a canonical switching cell and proved that they are electrically equivalent. He claimed that the Cuk converter exhibits no advantages over the conventional Buck-Boost converter (11). In the same year, Wood stated that switching converters should be classified and related by circuit function and not by circuit topology. Furthermore, he claimed that the Cuk converter is nothing more than the electrical reciprocal of the conventional Buck-Boost converter. Neither Landsman nor Wood provided a detailed comparison and evaluation of the performances of these two functionally equivalent and competitive converters. The claims made by Cuk about the advantages of his converters were based upon a comparison between the two converters using the same component values and switching frequency (13).

The drawback of the comparison made by Cuk is that these two converters did not satisfy the same performance specifications. Consequently, his conclusions about the superiority of the Cuk converter cannot be fully justified. Instead of using the same component values for the two converters, the comparison should have been based upon the optimum designs for a given set of performance specifications. Such a comparison will be made later in this dissertation.

(2) Motivation for the evaluation of coupled inductor Cuk converter under the balanced and unbalanced current ripple reduction

After the disclosure of Cuk converter in 1977, the coupled-inductor version of Cuk converter was introduced to further reduce either the input or output current ripples by coupling the input and output inductors on the same core, thus further reducing the size and weight. Depending on the relationship between the coupling coefficient and the turns ratio, the input and output current ripples can be equally reduced (balanced ripple reduction) or steered to either the input or the output (unbalanced ripple reduction). Cuk, based on the theoretical work (14,19,20), predicted the balanced and unbalanced current ripple reduction of this converter as a function of the coupling coefficient and the effective turns ratio of the coupled-inductor version of Cuk converter. No quantitative evaluation was made between these two modes of operation. In this research work, detailed comparisons and evaluations are made of these two modes of operation.

A block diagram that outlines the procedure for the comparisons between these two converters is given in Figure (1.1-2). Nonlinear

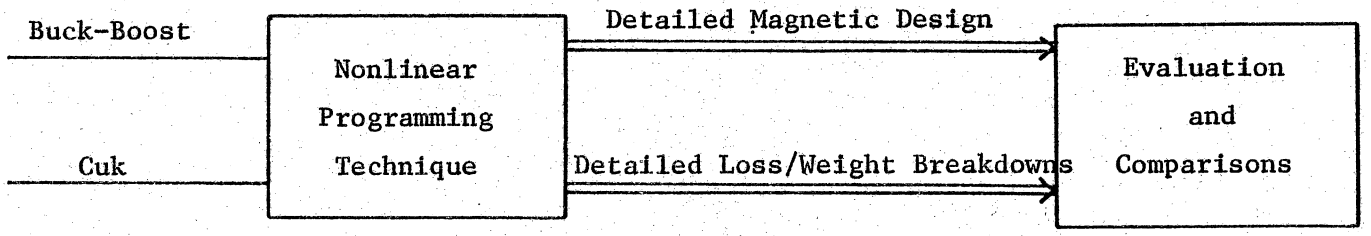

Figure (1.1-2) Block Diagram for the Evaluation and Comparisons of the Two Converters

programming (23) is utilized to calculate the detailed magnetic design information and the loss/weight breakdowns of the optimum designs of these two converters for a given set of performance specifications. The information thus obtained is then used for the comparison/evaluation of these two converters and the implementation of the complex magnetic components such as the inductors. The detailed magnetic design information includes the core size, wire size and the number of turns. The manufacturer's core catalog is then used to implement the design. In order to make the magnetic design realizable, a core gap may have to be incorporated. The information required to determine the optimum designs of these two converters includes:

(1) The design constants, such as, copper and core density, transistor and diode switching times, etc.

(2) Performance requirements, such as, input and output voltage level, output voltage ripple factor, input filter peaking limit, etc.

(3) Design constraints, such as, loss constraint, output ripple factor constraint, and maximum operating flux density constraint, etc.

(4) Objective function--the objective function is the quantity which is to be minimized, the quantity could be the total converter weight, loss, or cost. In the comparison of the two converters, minimum weight is the quantity to be achieved. The detailed nonlinear programming aspect utilized for the comparison will be elaborated upon in Chapter Three.

1.2 Review of Literature on the Development and Analysis of Switched-Mode Power Converters

The search for a more efficient way of obtaining DC power at various voltages to operate electronic circuits and equipment started more than a decade ago. In 1966, Moore and Wilson (24) laid the pioneering framework for a meaningful definition of DC to DC power conversion by summarizing, from a power-conditioning viewpoint, certain information on nonlinear circuit theory. In this paper, several constraints encountered in all DC to DC conversion networks were pointed out, including:

(1) the necessity of DC to AC inversion as an intermediate step within a DC to DC conversion network;

(2) the minimum amount of AC power which must be involved in this intermediate step; and

(3) the requirement for any network in which DC to AC inversion takes place to contain one or more active resistors which are properly connected in relation to the DC source.

In 1968, Kossov (25) derived the output-to-input voltage relationship as a function of duty cycle ratio and the output characteristics for the three basic converters--Buck, Boost, and Buck-Boost, for both the continuous and discontinous current modes of operation. Based on the work by Moore and Wilson, Hoo (26), in 1972, derived the general laws of DC-DC regulators independent of circuit topology and device physics. Hoo pointed out in this paper that the speed of regulation and possible size reduction of the energy storage devices within the regulator favored a high internal AC frequency. However,

this resulted in higher losses. He also pointed out that for a given set of requirements and a list of available devices, an absolute optimum design was extremely difficult to achieve since such factors as efficiency, cost, weight, and volume were in conflict. The lack of proper modeling and design tools was the cause of not achieving optimum converter design.

At this stage, the modeling of nonlinear switching power converter was still lacking. This situation started to change in 1972 when Middlebrook and Wester (27,28) introduced for the first time the Averaging Technique to model the switching regulator power stage for the continuous current operation. Simple analytical expressions in terms of circuit parameters were derived for the characteristic transient and frequency response for use in designing and understanding the behavior of switching converter power stages. The modeling of the highly nonlinear switching converter power stage subsystem was now available through the invention of the Averaging Technique. However, the modeling of the feedback modulator subsystem, which controls the switching of the power transistor of the power stage and which involves both analog and digital signal processing was still missing. This rendered the modeling of the entire switching regulator system composed of both the power stage and modulator subsystems incomplete.

In the same year, Middlebrook used the describing function method (DF) (29) to derive the transfer function for a constant frequency, variable duty-ratio, push-pull magnetic modulator employing square-loop cores (30,31). With the modeling and analysis of the power stage and feedback modulator subsystems available at this stage,

the behavior, such as, stability, transient response, output impedance and audiosusceptibility of a complete switching regulator could be analyzed and understood for the first time. Since then, this modeling technique has been applied to stability analysis and design of two-loop (32,33,34) and multi-loop (35) pulse-width-modulated (PWM) controlled DC/DC regulators in continuous and discontinuous current modes.

Then in 1975, Middlebrook described an experimental method to measure the loop gain of a closed-loop system by a voltage or a current injection technique without opening the loop. The important feature of this method was that the loop remained closed, so that waveforms of the operating points were not disturbed. This experimental method, coupled with the describing function method, permitted the analysis and design of switching regulators. The averaging technique is based on equivalent circuit manipulations, resulting in a single equivalent linear circuit. The averaging technique, unfortunately, is not general and unified for switching converter power stages.

In 1976, Middlebrook and Cuk coupled the state-space representation of switching networks with the equivalent circuit representation of the previously developed Averaging Technique resulting in a new State-Space Averaging Technique (21,22). This technique offered the advantages of both existing methods--the general unified treatment of the state-space approach, as well as an equivalent linear circuit of the averaging technique. With this new technique, any DC-to-DC switching converter can be modeled by a canonical circuit form (21). This canonical circuit model can be easily incorporated

with the feedback network into an equivalent circuit model of a complete switching regulator to study its dynamic and frequency response.

The benefits of significantly higher efficiencies and smaller sizes and weights of switched-mode regulators in comparison with conventional linear dissipative regulators are not achieved without a price; that is, the regulator input current has a substantial ripple component at the switching frequency, with a consequent necessity for an input filter to smooth out the current drawn from the unregulated line supply. The incorporation of an improperly designed input filter with a switching power converter can cause many problems. Yu pointed out that under certain conditions the filter-regulator combination can act like a negative resistance oscillator rather than a DC to DC converter (36). Sokal (37), in a more clear statement, derived a simple formula that predicted the oscillation of the filter-regulator system. At the same time, he also presented techniques to prevent the oscillation. Systematic investigation of the effects of the input filter on the stability of a switching regulator did not come until 1976 when Middlebrook applied the stage-space averaging technique to develop a design criteria for the filter-regulator combination (38,39).

At this stage, the modeling, analysis, and design of switching regulators were complete. But the search for new and more efficient converters went on. In 1976, Harada and Matsuo introduced the concept of cascaded connection of switching converters (40,41). In this concept, a new cascaded converter with a small duty-cycle ratio and a large regulation range as well as no

occurrence of switching surge was obtained. In the next year, 1977, Cuk, from the modeling and analysis point of view and the drive to derive a novel switching converter with both input and output non-pulsating currents, cascaded the boost converter by the buck converter and came out with a new converter which he claimed was the optimum topology for switching DC-DC power converters (13). In the following year, a coupled-inductor version of this new Cuk converter was disclosed in IEEE Industry Application Society Annual Meeting (14). This coupled-inductor version of a Cuk converter could reduce both the input and output current ripple as well as steering the zero current ripple to either the input or output side (19). In 1978, isolated single and multiple output versions of the Cuk converter were disclosed. These new versions of the Cuk converter are characterized by good self and cross regulations (14,15,42,43). In the same year, applications of the Cuk converter to the spacecraft battery, charging and discharging (16), and to high-frequency switched-mode power amplifiers (17) were reported.

With the modeling, analysis and design technique now available, the development of the switching regulator seems to be complete, however, this is not the case. A review of the components required to build a high frequency switching regulator reveals that, other than the control loop, there are four basic types of components which determine the overall power circuit stage performance. They are: the power switch, the magnetic components, the diode, and the capacitor. With the higher power, higher speed semiconductor devices and the large number of protective circuits now available,

the design of the magnetic components affects overall performance more than any of the other components. The various magnetic components being used in high frequency electronic power conversion today can be grouped into two major categories: transformers and inductors. The design details are quite complicated, including the core dimension, choice of core material, number of turns and the winding size as well as the problem of nonlinearities arising from magnetic saturation.

In 1972, Owen and Wilson (44) developed a series of programs for the design of the inductors of single-winding flyback converters. The programs searched an array of available core sizes and permeabilities for a complete list of windable cores that matched all constraints of the design equations. The design through this search was iterative and never reached the optimum design. In 1976, Owen and Wilson (45) improved the previous method by a screening rule that was based on the energy transfer requirement of the magnetic core (46). Using this screening rule, the search process was reduced to a methodical table search. Again, this was an iterative trial-and-error process, and the optimum design was never reached. In the following year, Judd and Kressler (47) presented a technique for designing transformers with given size and type of structure to have the maximum volt-ampere output while at the same time satisfying a number of design constraints. This technique was based on a mathematical optimization problem whose solution is a set of parameters characterizing the maximum VA output design. An assumption was made, such as, all dimensions of a given core geometry retained the same scale

to one another, in order to get analytic solutions. The distinguishing feature of this method was that it did not go through the iterative process as all previous methods did, and the optimum design was obtained in an attempt to minimize one objective function such as the power output of the devices. In this dissertation work, a powerful and efficient Nonlinear Programming technique will be used to determine the optimum magnetic design, without going through the iterative processes, and to facilitate the comparisons between the conventional Buck-Boost and the new Cuk converters. The comparisons made between these two converters under the optimum magnetic design are thus justified.

1.3 Outline of the Objectives

The previous two sections pointed out the controversy surrounding the performance of conventional Buck-Boost versus the new Cuk converters as well as previous work in the design and analysis of such converters. The research presented in this dissertation will mainly focus on the relative performance of the optimum conventional Buck-Boost and Cuk converters to a given set of performance specifications. The bases and procedures followed for these comparisons are summarized below:

1. The transistor switching frequency is held constant and the loss and weight breakdowns of the optimum designs for that frequency of the two converters are determined. This process is repeated for a range of frequencies which allow the determination of the loss/weight breakdowns as a function of the frequency. In this work, the frequency ranges from 20 KHZ to

60 KHZ in 10 KHZ steps. Several distinctive advantages can be realized by using this approach, namely:

a. By treating the frequency as a constant in each computer run of both converters, the program can be brought to faster convergence.

b. The comparison of the loss and weight breakdowns of both converters as a function of frequency can be clearly pictured. Most important of all, the optimum frequency range of both converters can be identified.

c. The tradeoffs between weights and losses of both converters as the frequency increases can be evaluated readily.

2. Next the switching frequency is treated as an unknown variable which is determined by Nonlinear Programming for both converters, such that, the optimum designs for a given set of performance specifications are obtained. Comparisons of these two converters, for the optimum designs, can then be made. Two advantages are gained through this approach, namely:

a. By treating the switching frequency as a variable, the overall design can be accomplished in one attempt without going through the laborous constant frequency approach as outlined in (1) or any other trial-and-error iterative processes resulting in a piece meal suboptimum design.

b. Comparisons of the results obtained under (1) and (2) can be checked against each other. For example, the optimum switching frequency from approach (2) can be checked to see if it falls near the valley or optimum frequency obtained from the constant frequency approach.

3. The optimum magnetic designs of the inductors for both converters are realized by the closest available cores from standard core catalogs to check if the magnetic designs of both converters are economically feasible. Otherwise they would have to be custom made.
4. Examine the merits of the coupled-inductor Cuk converter under balanced and unbalanced reduction of input/output current ripples.
5. Study the general profiles of loss and weight breakdowns of both converters as a function of switching frequency.
6. Study the switching device stresses of both converters. This study is important for the selection of reliable semiconductor switching devices.
7. Study the effect of the performance requirements on the Cuk converter design, such as the effect of EMI requirement, output voltage ripple factor, input voltage selection and the maximum operating flux density, on the total weight and loss profiles. This sensitivity analysis can provide some insights into global optimum converter design.
8. Study the impacts of magnetic loss and weight breakdowns on the total converter design.

CHAPTER 2

ANALYSIS OF THE CONVENTIONAL BUCK-BOOST CONVERTER AND THE CUK CONVERTER

It is well known that the Buck, Boost and Buck-Boost converters are the simplest switching converters to realize DC-to-DC voltage conversion. The Buck converter steps down the input voltage, the Boost converter steps up the input voltage, while the Buck-Boost converter can either step up or step down the input voltage depending on the switching duty cycle ratio. The three basic converters and their functions are shown in Figure (2.0-1), where symbol D represents the duty cycle ratio of the converter and is defined as the ratio of the transistor on time to the total on/off time or switching period.

However, the three converters all have the serious drawback of pulsating currents in either the input or the output side or both. For example, pulsating current is found on the input side of the Buck converter and on the output side of the Boost converter. It is no surprise that pulsating current is found in both the input and output sides of the Buck-Boost converter since it is the cascaded connection of the Buck converter followed by Boost converter. Consequently, the Buck-Boost converter inherited the undesirable properties of both converters.

The pulsating current on either the input or output side of the basic switching converters can cause serious electromagnetic interference or EMI problems on both the input and output sides or

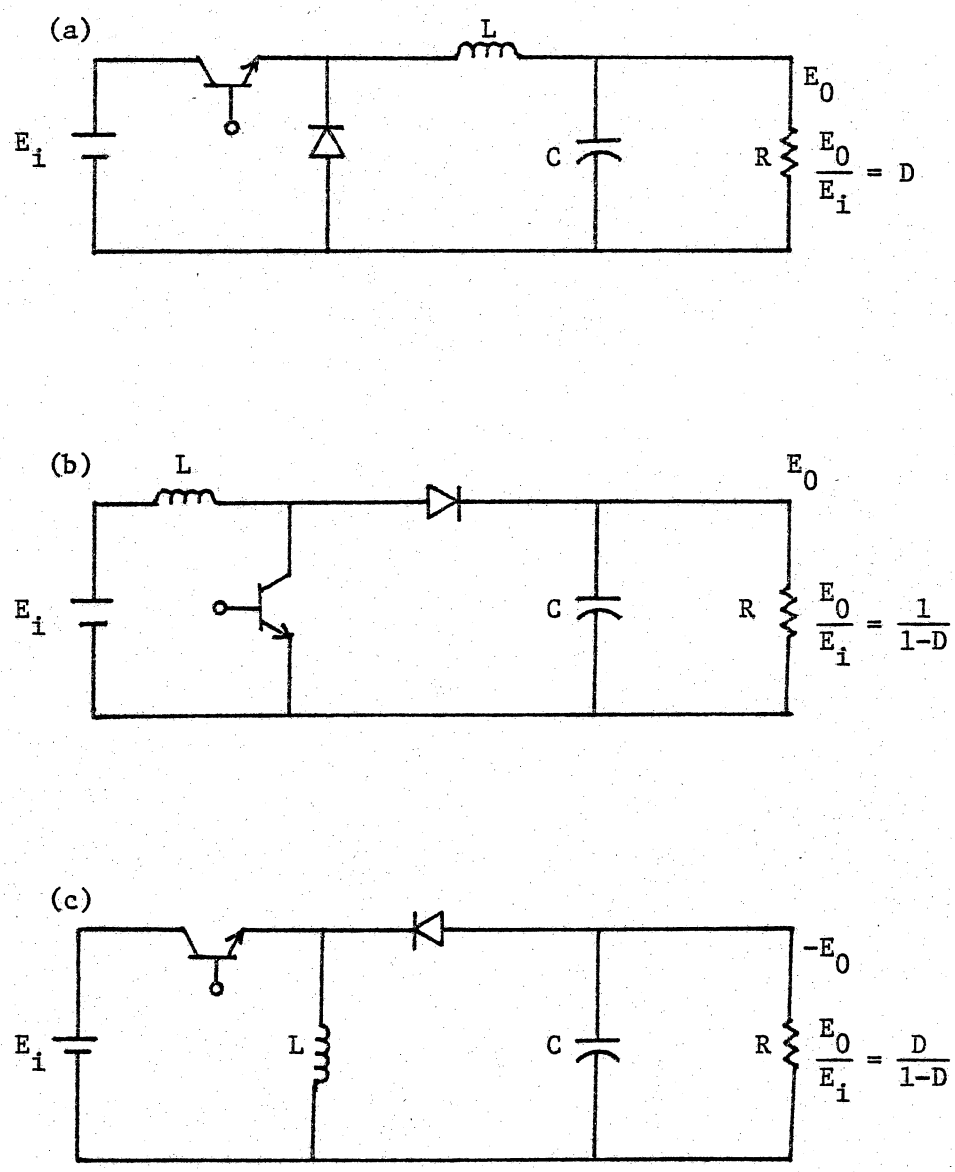

Figure (2.0-1) Three Basic Switching DC-DC Converters

(a) Buck
(b) Boost
(c) Buck-Boost

too high of an output voltage ripple. Another problem caused by the pulsed input current is that the DC input source cannot supply such pulsed current efficiently. Consequently, input and output filters are needed in the above three basic converters.

The invention of the Cuk converter was motivated by the objective to combine the desirable properties of the existing basic converters, that is, to cascade the desirable nonpulsating input current of Boost converter by the nonpulsating output current of the Buck converter as shown in Figure (2.0-2). Another desirable property of cascading the Boost by the Buck converter is that the general DC conversion property (both increase or decrease of the input voltage) is preserved as shown in Figure (2.0-2C). This configuration can either step up ($D > 0.5$) or step down ($D < 0.5$) the input voltage, depending upon the duty cycle ratio D.

It has been shown that the conventional Buck-Boost and the new Cuk converter are both formed by the cascaded connection of the existing basic Buck and Boost converters, the only difference being the cascading sequence. It is also interesting to note that these two converters are duals of each other as shown inside the dotted line in Figure (2.0-3). Although there are only minor topological differences between these two converters, the overall performance is quite different as will be brought out in Chapter 4 where detailed comparisons of the loss and weight breakdowns of the respective optimum design of these two converters are made.

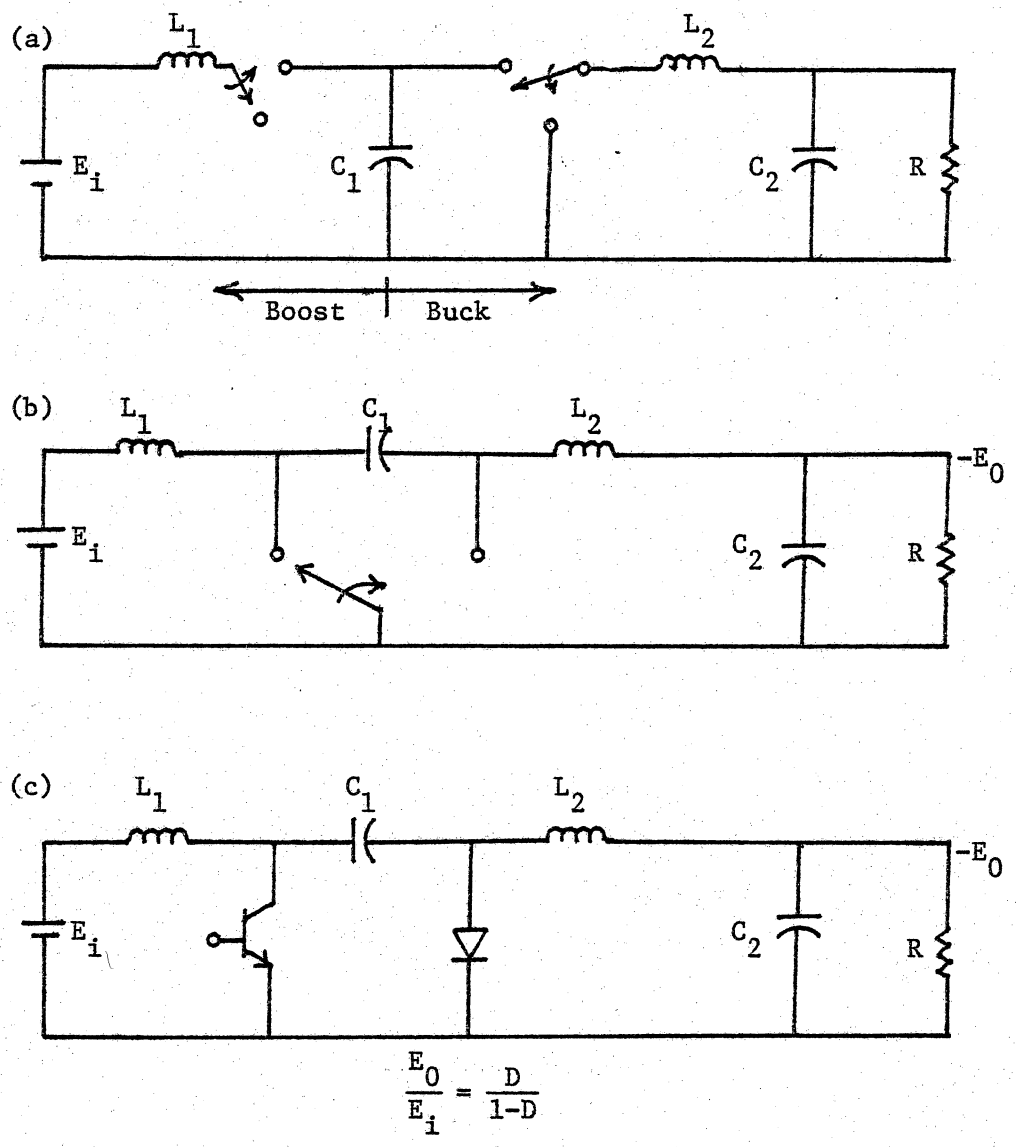

Figure (2.0-2) (a) Boost Cascaded by Buck Converter
(b) Transformation to New Cuk Converter
(c) Hardware Realization of the Switching Devices

(a)

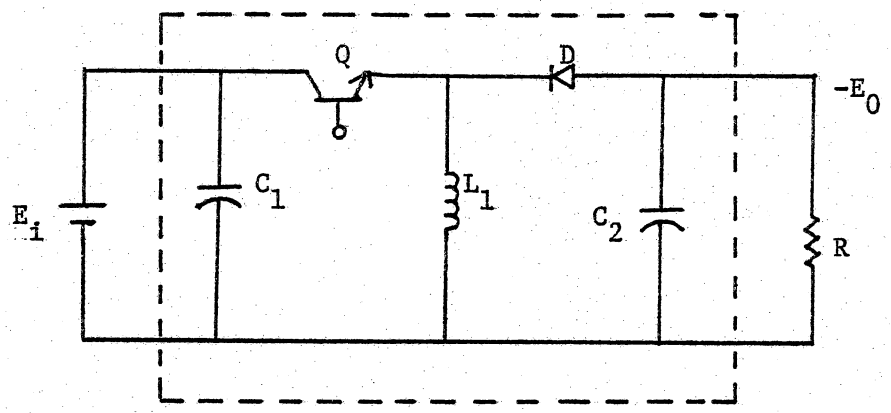

(b)

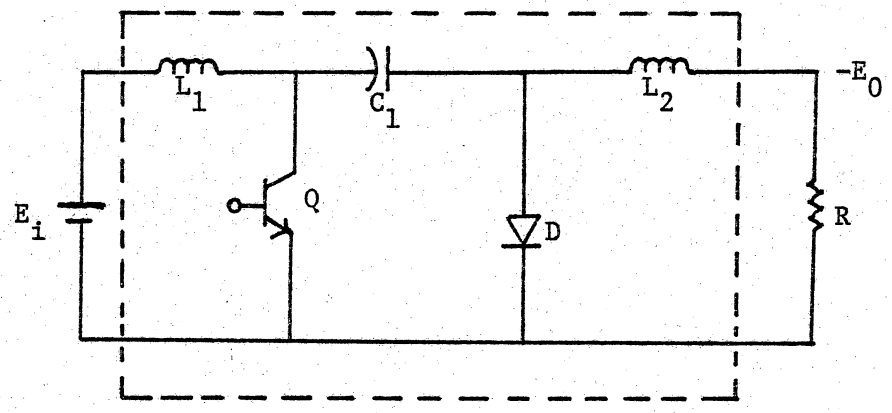

Figure (2.0-3) Duality of Buck-Boost and Cuk Converter

(a) Buck-Boost Converter

(b) Cuk Converter

2.1 Principles of Circuit Operation of the Two Converters and Waveforms

The research work done by Yu and Biess in 1971 on design aspects concerning input filter for DC-DC converters (36) had pointed out that the two-stage input filter provided the best compromise among many conflicting implications due to various filter requirements. The single-stage filter often cannot satisfy the specified requirements on audio susceptibility and is even bulkier than the two-stage filter (48). For these reasons, the two-stage input filters are incorporated in the comparisons of the conventional Buck-Boost and Cuk converters. Schematics of the final form of the conventional Buck-Boost and Cuk converters which are used for the comparisons and evaluations are given in Figure (2.1-1) and Figure (2.1-2) respectively. The unknown design variables that characterize the performance of these converters are also given in these figures. The unknown design variables are determined for a given set of performance specifications by means of a nonlinear programming technique which will be discussed later in this dissertation.

2.1.1 Principles of Circuit Operation of the Buck-Boost Converter

The conventional Buck-Boost converter as shown in Figure (2.1-1) is constructed by four ingredients:

1. The two stage input filter composed of L_1, L_2, C_3, C_4.
2. One power transistor switch and one commutating diode.
3. The energy storage/transfer inductor L_6.
4. The output filter C_5.

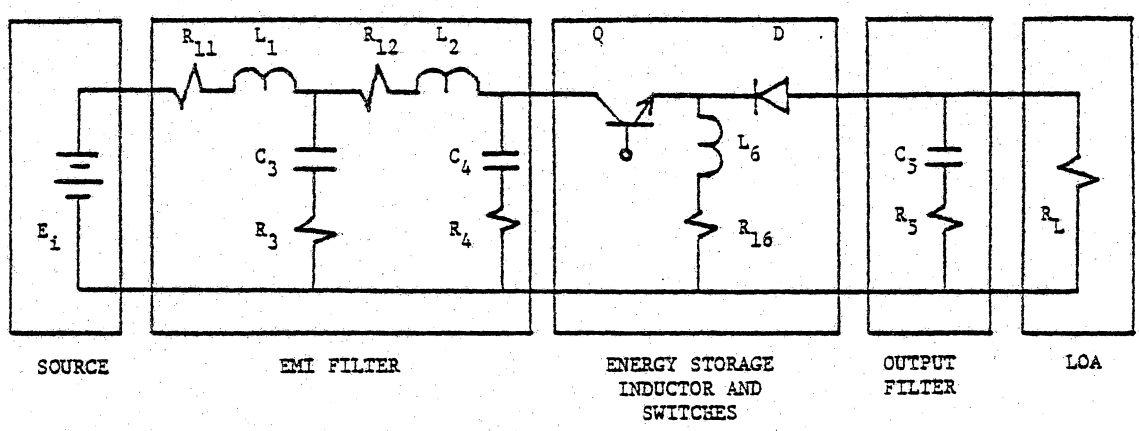

DESIGN UNKNOWNS: 24 VARIABLES

R_{11}, R_{12}, R_{16}	:	Parasitic Resistances of Inductors
R_3	:	EMI Filter Damping Resistor
L_1, L_2	:	EMI Filter Inductors
L_6	:	Energy Storage Inductor
C_3, C_4, C_5	:	Filter Capacitors
A_1, A_2, A_3	:	Core Cross-Section Area
Z_1, Z_2, Z_6	:	Mean Magnetic Path Length
N_1, N_2, N_6	:	Number of Turns of the Winding
A_{C1}, A_{C2}, A_{C6}	:	Winding Area Per Turn
F	:	Converter Operating Frequency
e	:	Overall Operating Efficiency

Figure (2.1-1) Conventional Buck-Boost Power Converter With Design Unknown Variables

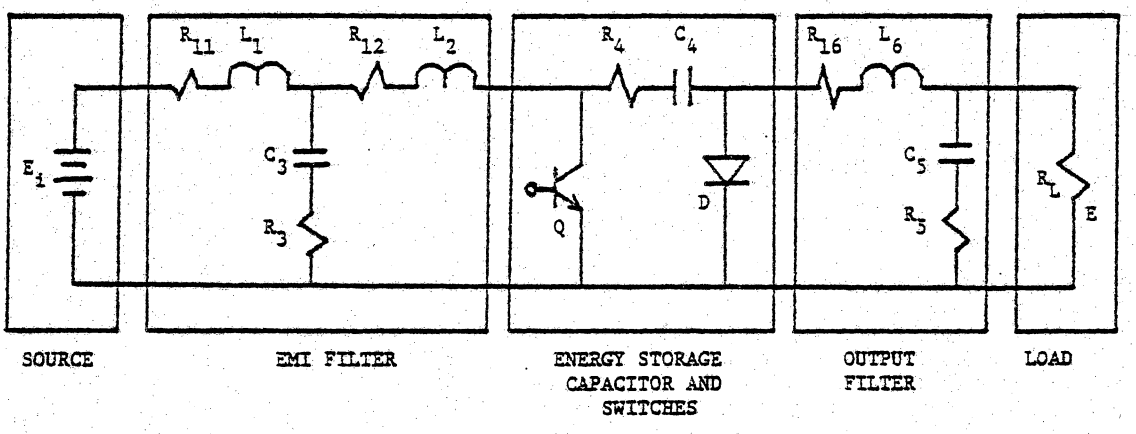

DESIGN UNKNOWNS: 24 VARIABLES

R_{11}, R_{12}, R_{16}	:	Parasitic Resistances of Inductors
R_3	:	EMI Filter Damping Resistor
L_1, L_2	:	EMI Filter Inductors
L_6	:	Output Filter Inductor
C_3, C_5	:	Filter Capacitors
C_4	:	Energy Storage Capacitor
A_1, A_2, A_6	:	Core Cross-Section Area for a Given Magnetic Material
Z_1, Z_2, Z_6	:	Mean Magnetic Path Length
N_1, N_2, N_6	:	Number of Turns of the Winding
A_{C1}, A_{C2}, A_{C6}	:	Winding Area Per Turn
F	:	Converter Operating Frequency
e	:	Overall Operating Efficiency

Figure (2.1-2) Cuk Converter with Design Unknown Variables

All of the resistances of this circuit except for R_3 which is used as a damping resistor and R_L which represents the load, are parasitics of their respective devices.

The input electromagnetic interference (EMI) filter serves two purposes. (1) It solves the audio susceptibility problem. That is, it isolates the regulator from the input source voltage variations and the unexpected transients which may appear at the input to the converter. (2) It solves the electromagnetic interference (EMI) conducted current problem (49-54). That is, it suppresses the switching alternating current component, generated by the transistor switching action, from being reflected back to the source that may interfere with the source or other loads hanging on the same source.

The power transistor, which is used as a switch, is responsible for the DC to AC inversion as an intermediate step necessary in a DC-DC switcher. The output filter is needed to eliminate harmonics in the output DC voltage due to the transistor switching.

The detailed circuit operation can be better understood by breaking down the original circuit into two circuit configurations corresponding to the on and off states of the power transistor as shown in Figure (2.1-3). The critical circuit waveforms of the circuit are also shown in detail in Figure (2.1-4) to help explain the principles of the converter operations.

(1) <u>The interval DT when the transistor is on</u>

The circuit configuration corresponding to this interval is shown in Figure (2.1-3a). Starting with the input filter operation; the first stage, consisting of L_1, C_3, R_3,

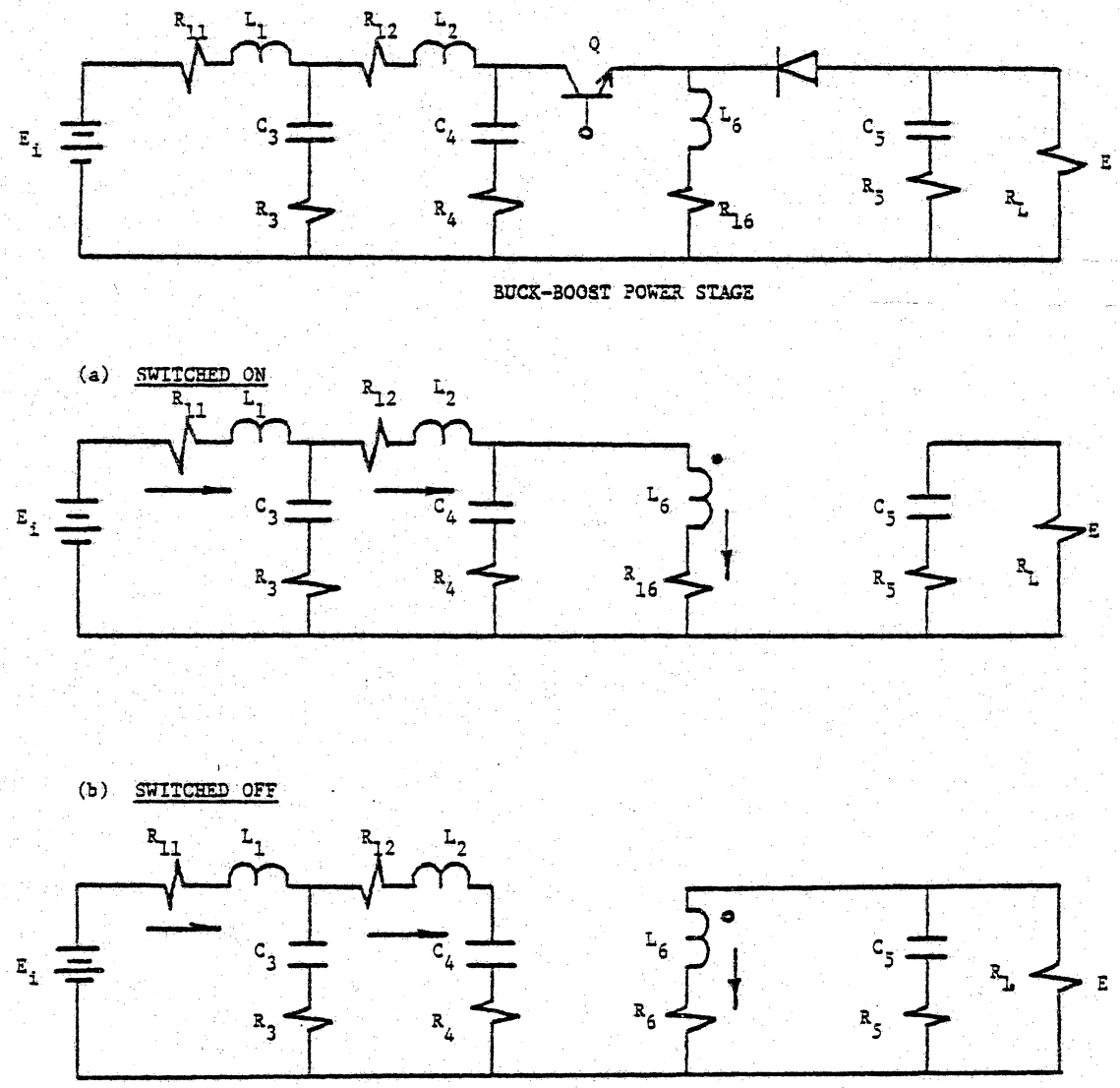

Figure (2.1-3) Buck-Boost Circuit Configurations During the Two Switching Intervals

controls the resonant peaking of the filter, R_3 is built in to set the Q-factor to be not greater than some specified value in order to control the damping. Also in order to avoid the power loss in the shunt damping resistor, R_3, a blocking capacitor, C_3, is placed in series with it. The second stage of the input filter consists of L_2, C_4 which supply most of the pulsed current demanded by the power switch when it is on. Since C_4 provides essentially most of the pulsed current, negligible current flows in C_3 and R_3, and inductor L_1 passes essentially a direct current required by the power converter. Since C_4 supplies the pulsed current, a low ESR (equivalent series resistance) capacitor is highly recommended in order to reduce the ESR loss. During this interval, the ramp current through the transistor i_Q charges the energy storage/transfer inductor L_6 as shown in Figure (2.1-4) ready for discharging to the output filter and load in the next off interval. The commutating diode is reversed biased and cut off during this interval and consequently the energy stored in the output filter capacitor is discharged to supply the load current.

(2) <u>The interval (1-D)T when the transistor is off</u>

The circuit configuration corresponding to this interval is shown in Figure (2.1-3b). Some differences can be observed by inspecting the circuit waveforms shown in Figure (2.1-4). First, the input current charges the filter capacitor C_4 to compensate for the energy discharged in the previous on

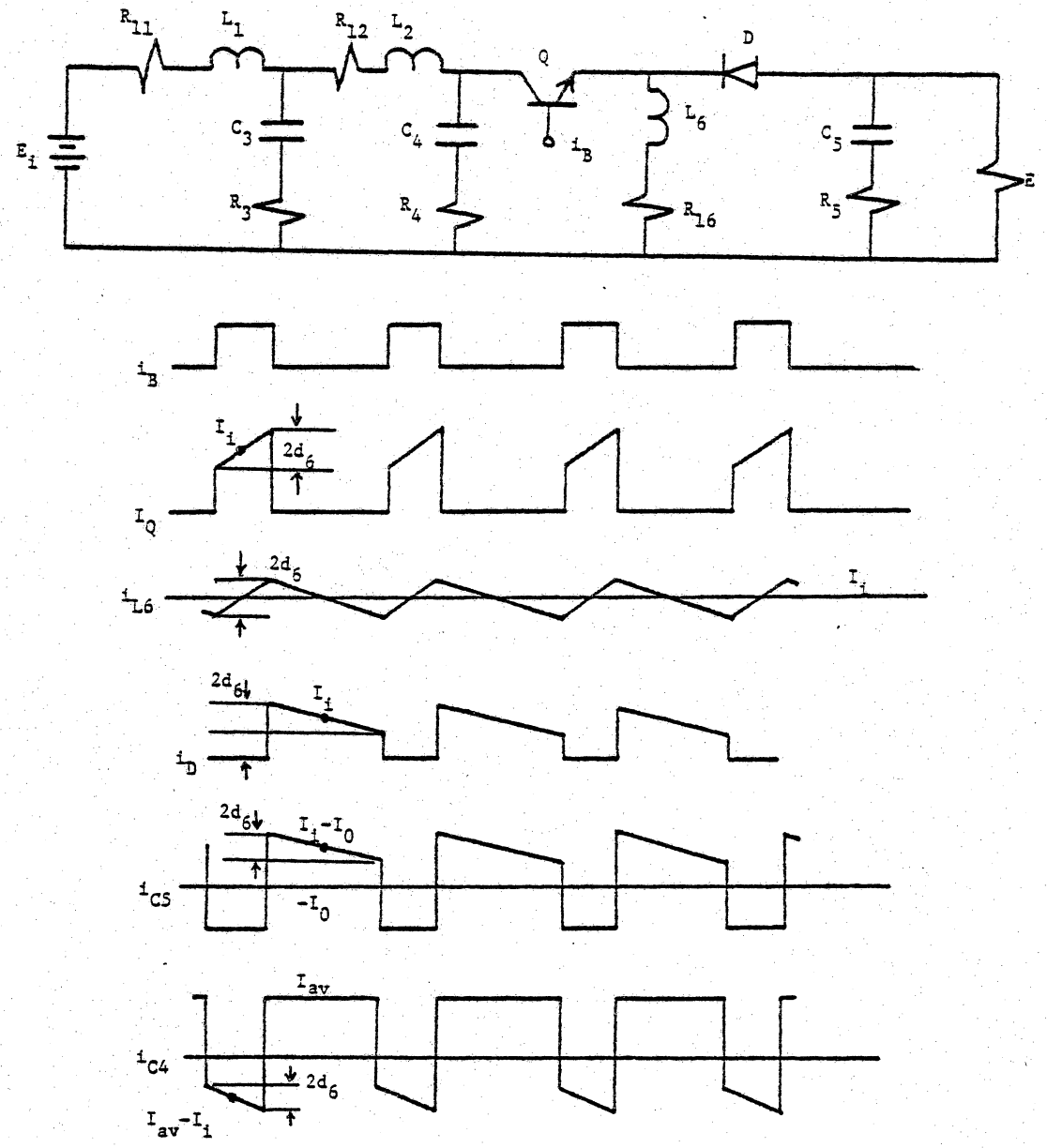

Figure (2.1-4) Critical Circuit Waveforms of the Conventional Buck-Boost Converter

state. Second, the commutating diode is an automatic switch in that it closes when the transistor is open in order to commutate the continuous energy storage/transfer inductor current i_{L6}. Third, the energy stored in the energy storage/transfer inductor in the previous state now discharges to supply the load current and recharges the output filter capacitor C_5. The energy discharged from energy storage/transfer inductor in this off state can be depicted by the ramp down inductor current i_{L6} shown in Figure (2.1-4).

(3) The circuit waveforms shown in Figure (2.1-4) are not only used to understand the circuit operation of the converter, but they are also used to derive some of the design constraints as will be shown in the following sections. The designations used to represent the current quantities in Figure (2.1-4) and the input-output voltage relationship are summarized in the following:

a. Input-Output Voltage Relationship:

$$\frac{E_o}{E_i} = \frac{T_{on}}{T_{off}} = \frac{D}{1-D} \qquad (2.1\text{-}1)$$

where T_{on} = Transistor on time

$T_{off} = T - T_{on}$

D = Duty cycle ratio $= \frac{T_{on}}{T}$

(b) i_B = Pulse current for transistor base drive

I_i = Average DC current of the transistor current pulse

$$= \frac{P_o}{eE_i} \frac{T}{T_{on}} = \frac{P_o}{eE_i} \frac{E_o + E_i}{E_o} \qquad (2.1\text{-}2)$$

I_{av} = Average DC current drawn from the source

$$= \frac{P_o}{eE_i} \qquad (2.1\text{-}3)$$

$2d_6$ = Peak-peak AC current ripple through the transistor

$$= \frac{E_i E_o}{(E_o + E_i)L_6 F} \qquad (2.1\text{-}4)$$

I_o = Average DC output load current

(c) It is important to point out at this stage two important factors concerning the circuit waveforms of the conventional Buck-Boost converter. (i) The current through the transistor is discontinuous. In order to make the average current in the input and output ports of the two stage input filter equal, the average current of the discontinuous transistor current pulse I_i is T/T_{on} times higher than the input average source current I_{av}. This higher current pulse flows through the energy storage/transfer inductor and causes a large power loss. This effect will be verified by the computed results given in Chapter 4. (ii) By inspecting the current waveforms through the output filter capacitor C_5 as shown in Figure (2.1-4), one can notice that the output voltage ripple of the conventional Buck-Boost converter is load-dependent. This

means heavier load current causes higher output voltage ripple. This can be remedied by using a larger filter capacitor with the accompanying heavier weight penalty. This load-dependent voltage ripple is caused by the discontinuous current through the commutating diode.

2.1.2 Principles of Circuit Operation of the Cuk Converter

The prominent features of Cuk converter and its basic circuit operation will be discussed in this subsection. Circuit features similar to the previous discussion for the conventional Buck-Boost converter are omitted. The salient feature of Cuk converter is that it uses capacitor as the energy storage/transfer device instead of the inductor as found in the existing switching converters. It must be stressed here that "energy storage/transfer" refers to the storage of the energy from the input port at one switching state and the transfer of that energy to the output port at the next switching state. Thus, it could be said that the energy storage/transfer device is responsible for connecting the input and output ports of any switching power converter. Without this connection, the switching DC-DC power conversion would not be possible. Again, the detailed circuit operation of Cuk converter can be understood by breaking down the original circuit into two circuit configurations corresponding to the on and off state of the transistor power switch as shown in Figure (2.1-5). The critical circuit waveforms are also shown in detail in Figure (2.1-6) to help explain the principles of the converter operations.

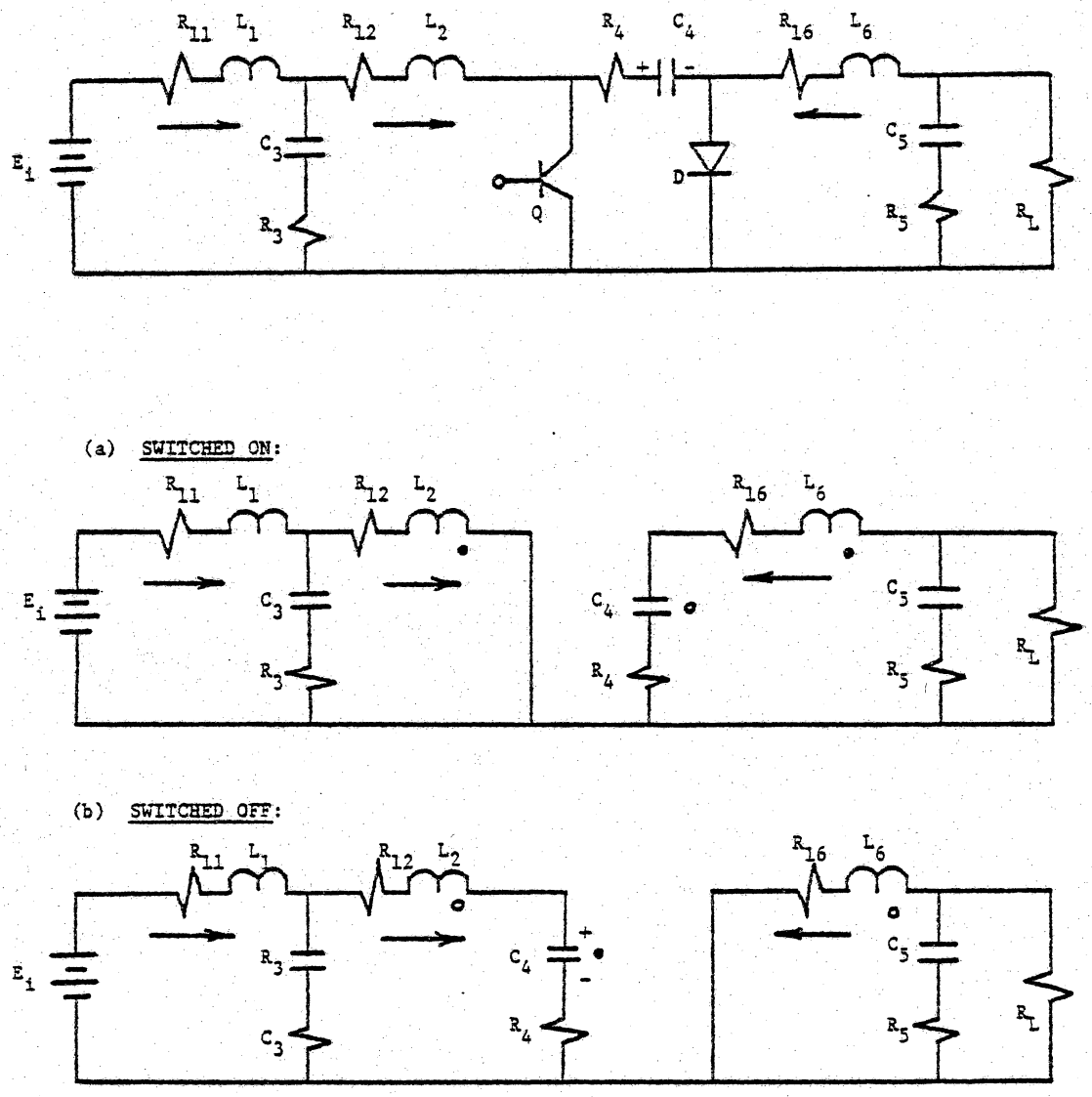

Figure (2.1-5) Cuk Converter Circuit Configurations During the Two Switching Intervals

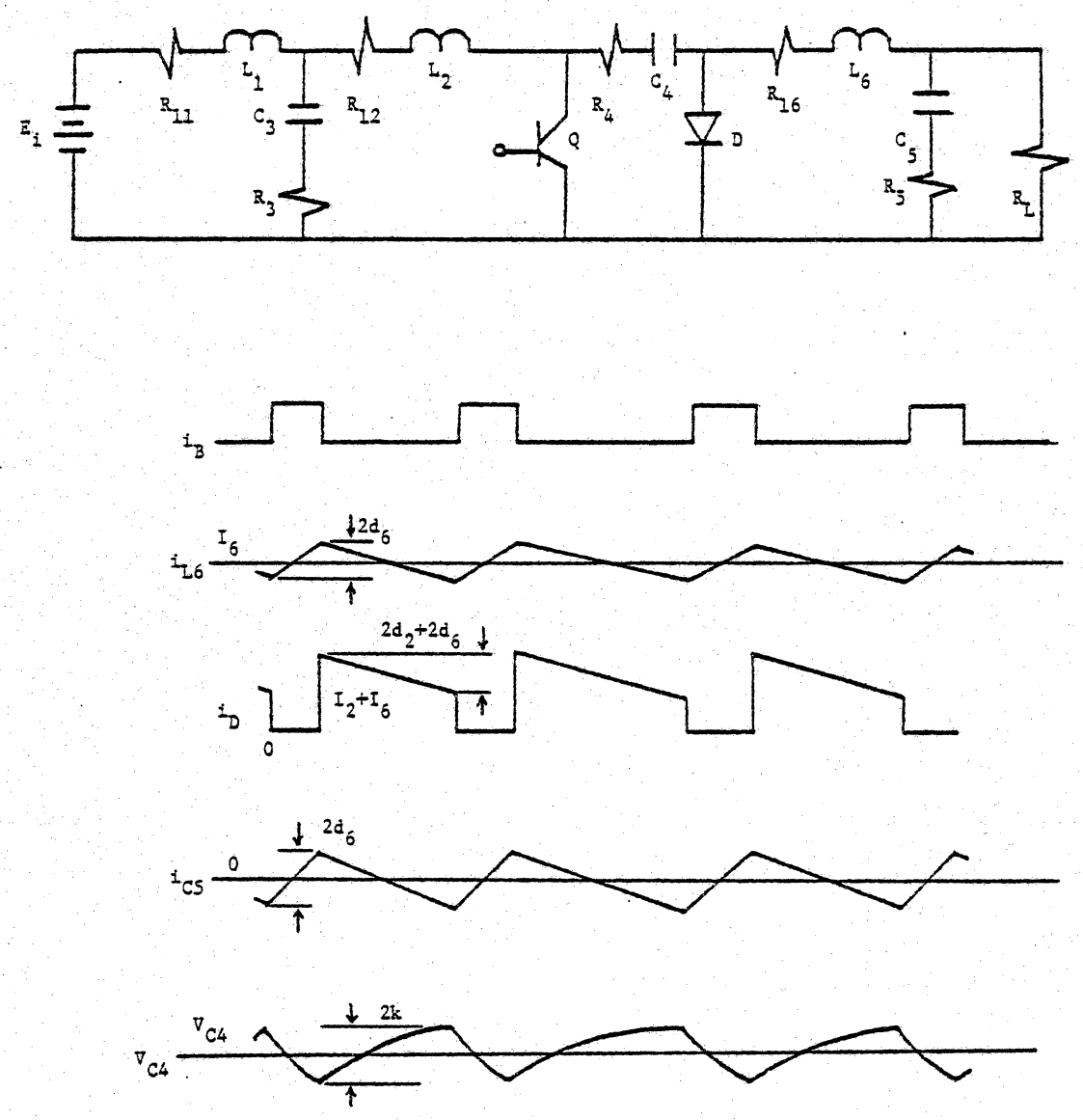

Figure (2.1-6) Critical Circuit Waveforms of the Cuk Converter

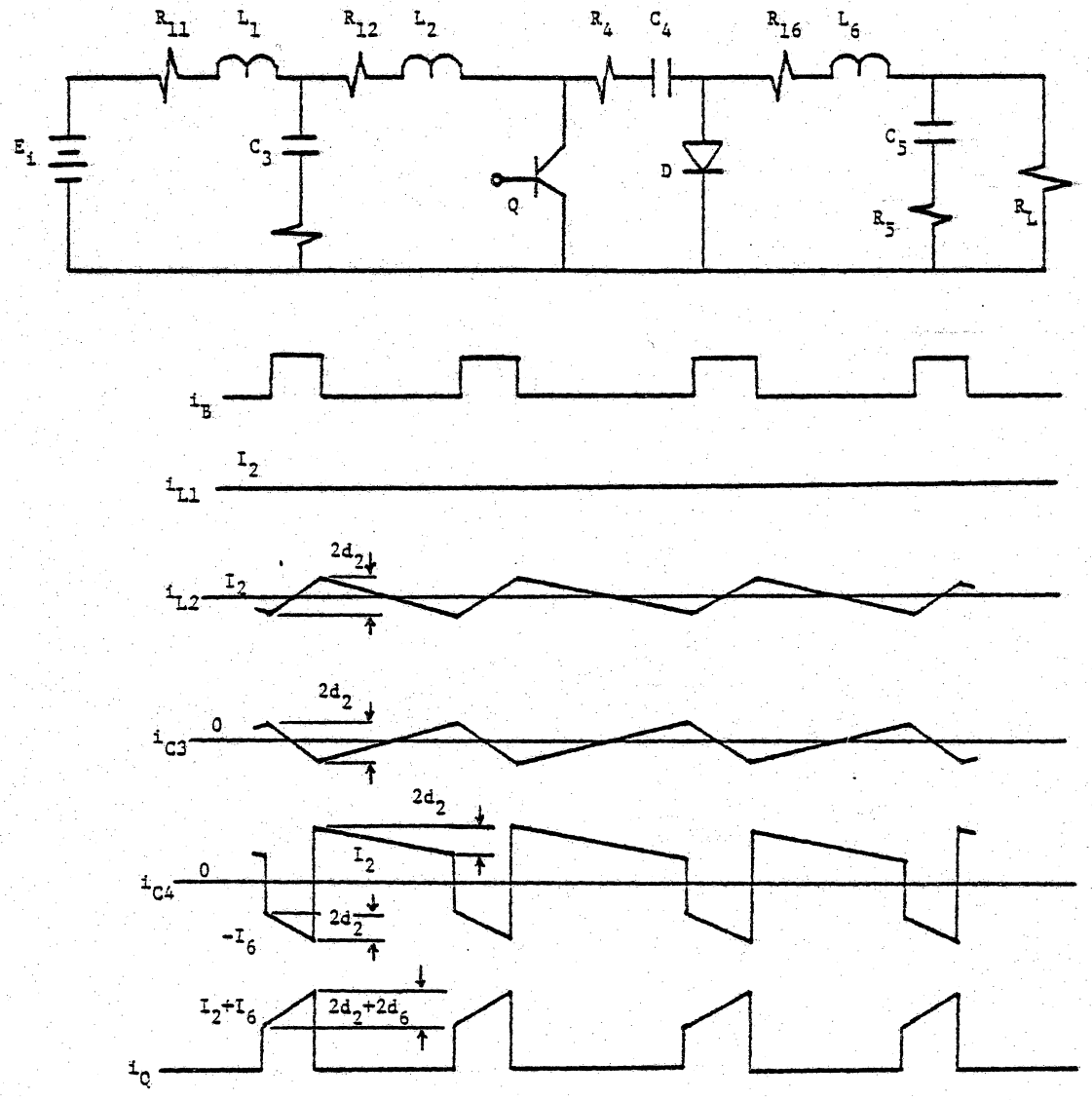

Figure (2.1-6) Critical Circuit Waveforms of the Cuk Converter (continued)

(1) The interval when the transistor switch is off

The operation of Cuk converter can be explained more clearly beginning with the interval when the transistor is off. Starting from Figure (2.1-5b) when the power switch is off, the diode is forward biased and the energy storage/transfer capacitor C_4 is charging in the positive direction, while the input filter inductor L_2 is discharging through the conducting diode. At the output port, the energy stored in L_6 is discharging to supply the load current and part of the energy of the filter capacitor C_5. Consequently, during the off state, the energy storage/transfer capacitor C_4 is connected to the input port and energy storage takes place.

(2) The interval when the transistor is on

The circuit configuration corresponding to this state is shown in Figure (2.1-5a). As soon as the transistor is turned on, positive voltage across the energy storage/transfer capacitor is connected across the diode, thus reverse biasing it which causes it to cut off. In this interval, the energy stored in C_4 during the previous interval is being discharged through the transistor to supply the load current and to charge the output filter capacitor C_5 and the filter inductor L_6. At the input port, the input current is charging inductor L_2 to compensate for the energy it discharges during the previous interval. Thus volt-seconds in the inductors and coulomb-charge in the capacitors are all balanced during a complete switching cycle.

(3) The designation used to represent the current quantities in Figure (2.1-6) and the input-output voltage relationships are also summarized in the following:

(a) Input-Output Voltage Relationship:

$$\frac{E_o}{E_i} = \frac{T_{on}}{T_{off}} = \frac{D}{1-D} \tag{2.1-5}$$

So the Buck-Boost and Cuk converter both have the capability of either stepping up or stepping down the input voltage depending on the duty cycle ratio D.

(b) I_2 = Average DC current through L_2

$$= \frac{P_o}{eE_i} \tag{2.1-6}$$

I_6 = Average DC current through L_6

$$= \frac{P_o}{E_o} \tag{2.1-7}$$

$2d_2$ = Peak-peak AC ripple current through L_2

$$= \frac{E_i E_o}{(E_o + E_i)L_2 F} \tag{2.1-8}$$

$$2d_6 = \frac{E_i E_o}{(E_o + E_i)L_6 F} \tag{2.1-9}$$

V_{C4} = Average DC voltage across C_4

$$= \frac{E_o}{D} \tag{2.1-10}$$

$2K$ = Peak-peak AC voltage ripple across C_4

$$= \frac{P_o}{2(E_o + E_i)C_4 eF} \tag{2.1-11}$$

(c) By examining the circuit waveforms of both converters, it is instructive to point out some interesting points concerning the two converters. (i) Only the input or output currents pass through the transistor or diode for the conventional Buck-Boost converter, while the diode and transistor in the Cuk converter carry the sum of input and output current. The average currents through the switching devices are compared in Table (2.1-1). Depending on the operating efficiency, it is not necessarily true that the currents through the switching devices of Buck-Boost converter are less than those of the Cuk converter. This may be the case even though there are two current components passing through the switching devices of the Cuk converter, because the magnitudes of these currents may be less than the counterparts of the conventional Buck-Boost. (ii) Due to the two inductors L_1, L_6 in the input and output ports of the Cuk converter, there are no pulsating currents in both ports. (iii) By inspecting the current waveforms through the output filter capacitor of the Cuk converter, it is noticed that the output voltage ripple of the Cuk converter is load-independent.

Detailed comparisons of loss and weight breakdowns of these two converters will be carried out in Chapter 4.

2.2 Descriptions of the Computer Model for Both Converters

As pointed out clearly in Chapter 1, the research work of this dissertation is mainly focused on the comparison and evaluation of the performance aspects of two very similar but topologically

Table 2.1-1

Comparisons of average currents through the switching devices of the two converters

	Buck-Boost	Cuk
Transistor	$\frac{P_0}{eE_i}\ \frac{E_0 + E_i}{E_0}$	$\frac{P_0}{eE_i}\ \frac{E_0 + eE_i}{E_0}$
Diode	$\frac{P_0}{eE_i}\ \frac{E_0 + E_i}{E_0}$	$\frac{P_0}{eE_i}\ \frac{E_0 + eE_i}{E_0}$

different converters, i.e., the conventional Buck-Boost and the newly disclosed Cuk converters. Before embarking on the computer implementation of the comparison and evaluation, all of the design information needed for the Nonlinear Programming Technique will be discussed first. The four sets of input information needed to be fed to the nonlinear programming package include the design constants, constraints, the performance requirements, and the optimization objective function desired by the customers. Usually the customers are most concerned about obtaining the best circuit which satisfies all of the performance specifications and constraints while at the same time minimizing or maximizing the objective function. For example, they may be concerned about minimizing the cost for commercial applications or minimizing the weight and volume aspects for aerospace applications.

In this work, the comparisons and evaluations of these competitive circuit configurations are based on the minimum weight aspect. The four sets of inputs needed for the computer implementation of the comparison are described in the following subsections.

2.2.1 Performance Requirements and Objective Function

These requirements are usually specified and demanded by the customers. In power converter power stage selection, the performance specifications include the input and output voltage, input filter design to fulfill the requirements of the FCC (Federal Communication Commission) regulation, such as, the EMI specification, and most important of all, the quality of the output voltage (53,54). The objective function evaluated in this work will be that of minimum weight which is of prime importance in aerospace applications. The

performance specifications and objective function are broken down as follows:

(1) Performance Requirements

PE1: EMI filter resonant peaking limit

P_o: Output power

E_i: Input voltage

E_o: Output voltage

S: Frequency dependent source conducted current interference limit

rf: Output voltage ripple factor

(2) Objective Function: Total weight of the converter

The objective function (or cost function) is the quantity which is to be minimized. It can be any physically realizable quantity, such as, cost, weight, size, and volume, etc. What is of concern here is the comparison of these two converters under the minimum weight aspect. Thus, the objective function will be the total weight of the converter; it is composed of the magnetic core and winding weight, capacitor weight, source weight, heat sink and packaging weight. Refer to Figure (2.1-1) and Figure (2.1-2) for the meanings of the symbols used in the following equation for the objective function.

WI = Core weight

$$= D_I(A_1Z_1 + A_2Z_2 + A_6Z_6) \qquad (2.2\text{-}1)$$

where AZ = core volume

WW = Winding weight

$$= 4F_C D_C \left(A_{C1} N_1 \sqrt{A_1} + A_{C2} N_2 \sqrt{A_2} + A_{C6} N_6 \sqrt{A_6}\right) \quad (2.2\text{-}2)$$

Where $4F_C A_1$ = Mean length per turn of the winding

WC = Capacitor weight

$$= D_{K3} C_3 + D_{K4} C_4 + D_{K5} C_5 \quad (2.2\text{-}3)$$

WS = Source weight

$$= \frac{P_0}{eK_S}, \text{ Where } \frac{P_0}{e} = \text{Input power} \quad (2.2\text{-}4)$$

WH = Packaging weight

$$= \frac{P_{0(1-e)}}{eK_H}, \text{ Where } \frac{P_0}{e} - P_0 = \text{Total loss} \quad (2.2\text{-}5)$$

$$\text{Objective Function} = WI + WW + WC + WS + WH \quad (2.2\text{-}6)$$

2.2.2 Design Constants

These design constants are obtained either through the designer's own experiences or through the manufacturer's catalog, data sheets and specifications. The collection of design constants needed for the comparison of the two converters is listed below:

F_C : Window pitch factor, ratio of one turn conductor average length to the core circumference

F_W : Core window fill factor, percentage of core window area actually occupied by the winding

ρ : Conductor resistivity

D_I	:	Core density
D_C	:	Conductor density
B_S	:	Maximum operating flux density
D_K	:	Weight per farad
V_{ST}, V_{BE}	:	Voltage drop across collector-emitter and base-emitter
T_{SR}, T_{SF}	:	Transistor switching times
V_D	:	Diode forward voltage drop
T_{ND}, T_{FD}	:	Diode switching times
T_{RE}		
K_H	:	Packaging weight density
K_S	:	Source weight density
K	:	Core window area dimensional ratio

2.2.3 General Discussions on Design Constraints

As pointed out in the previous sections, four constructing ingredients are needed to make a working switching power converter: input filter, switching devices, energy storage device, and output filter.

(1) The filter serves two functions: (a) to prevent the alternating current component generated by the switching devices from being reflected back to the input source to fulfill the regulations on EMI requirement by the Federal Communication Commission (FCC), and (b) to isolate line-voltage transients and ripple in the bus so as not to degrade the performance of the switching converter; this is to fulfill the line rejection requirement or audiosusceptibility requirement.

Consequently, the filter must provide high attenuation at the switching frequency and sufficient damping against the bus disturbances so that input filter peaking is controlled at the resonant frequency of the filter. The two-stage filter is capable of meeting all these requirements, i.e., high attenuation, controlled resonant peaking requirement, and low losses. Due to the above facts, there are two design constraints associated with the input filter design: (a) frequency dependent source conducted EMI constraint, (b) input filter peaking constraint.

(2) Design effort to keep the output voltage ripple as low as possible necessitates the incorporation of output filter for a switching converter. The control of ripple, both externally and internally generated, is a primary consideration of a good power supply. An appropriate output ripple factor fulfilling the needs is an integral part of the design effort.

(3) Efficiency is another important factor to be considered in a power supply design. Switching losses of the semiconductors operating at high frequency constitute one of the major losses. Thus, a loss constraint must be included as a necessary part of the system operation. The loss components in the switching converter can be identified as follows:

(a) The conduction and the switching losses of the semiconductor devices: the switching losses are calculated on the assumption of linear changes of voltage and current from their initial to final values, and the power loss is

the integral of the instantaneous product of voltage and current during the switching transition.

(b) Magnetic losses: they include the EMI filter winding losses and the energy storage/transfer core and winding losses.

(c) Capacitor ESR (equivalent series resistance) losses: they arise from the periodic charging and discharging of the filter capacitor energy storage/transfer capacitor.

(4) The final design constraints to be considered in a switching converter are concerned with the magnetic designs. The complicated facets of the magnetic design and its importance have been pointed out earlier in Chapter 1. Since magnetic components contribute a major portion of the overall converter weight, improper design, such as the wrong core size, number of turns and wire sizes, could cause a serious weight and loss penalty. Some of these complicated facets of the magnetic design are described below:

(a) Since the inductor components used in the two converters are supposed to operate in the linear region of the B-H characteristic, operation of the flux density in the saturation region could cause the malfunction of the converter operation (one immediate effect is that the energy could not be transferred). This limitation leads to maximum operating flux density constraints for the magnetic components based on the selection of materials available.

(b) In order to realize a core design, the core must be windable. Also, to save size and weight, the core window area must be minimized so that it just accommodates all of the windings.

This consideration leads to the core window area constraints.

(c) The core winding always contributes some resistance and power losses (copper losses), thus these parasitic effects are also considered as design constraints. All the design constraints and their sources of necessity in considering the switching power converter implementation are grouped in Table (2.2-1).

2.2.4 Design Constraints for Conventional Buck-Boost Converter

The design constraints of the conventional Buck-Boost converter are listed in this section and those of the Cuk converter are listed in the following section.

(1) Loss Constraint: $C(1) = 0$

$$C(1) = P_0(\frac{1}{e} - 1) - PIF - PQ - PD - PESR - POF - PESC$$

The loss constraint is an equality constraint, the first term in the above equation is the total loss, it is the sum of all the losses of the power converter. The loss components are shown in the following:

PIF = EMI filter power loss

$$= \left(\frac{P_0}{eE_i}\right)^2 (R_{11} + R_{12}) \qquad (2.2\text{-}7)$$

PQC = Transistor conduction loss

$$= \frac{P_0 V_{st}}{eE_i} \qquad (2.2\text{-}8)$$

PQS = Transistor turn-on loss + turn-off loss

Table (2.2-1)

Design Constraints and Their Sources of Necessity

(1) EMI input filter:

- Frequency dependent source conducted EMI constraint
- Input filter peaking constraint

(2) Switching devices and parasitics of components

- Loss constraint

(3) Output filter:

- Output ripple factor constraint

(4) Magnetic considerations:

- Core window area constraint
- Maximum operating flux density constraint
- Parasitic resistance constraint

$$= \frac{T_{sr}F}{6}(E_0 + E_i + V_d + 2V_{st})\left[\frac{P_0}{eE_i}\frac{E_0 + E_i}{E_0} - \frac{E_iE_0}{2(E_0 + E_i)L_6F}\right]$$

$$+ \frac{T_{sf}F}{6}(E_0 + E_i + V_d + 2V_{st})\left[\frac{P_0}{eE_i}\frac{E_0 + E_i}{E_0} + \frac{E_iE_0}{2(E_0 + E_i)L_6F}\right] \quad (2.2\text{-}9)$$

PQB = Transistor base drive loss

$$= \frac{0.1\ P_0V_{st}}{eE_i} \quad (2.2\text{-}10)$$

PQ = Transistor total power loss

= PQB + PQC + PQS

PDC = Diode conduction loss

$$= \frac{P_0V_d}{eE_0} \quad (2.2\text{-}11)$$

PDS = Diode turn-on loss + turn-off loss + recovery loss

$$= \frac{T_{nd}F}{12}\left[\frac{P_0}{eE_i}\frac{E_0 + E_i}{E_0} + \frac{E_iE_0}{2(E_0 + E_i)L_6F}\right][E_0 + E_i + 2V_d - V_{st}]$$

$$+ \frac{(T_{fd} + 3T_{re})}{12}\left[\frac{P_0}{eE_i}\frac{E_0 + E_i}{E_0} - \frac{E_iE_0}{2(E_0 + E_i)L_6F}\right]$$

$$[E_0 + E_i + 2V_d - V_{st}] \quad (2.2\text{-}12)$$

PD = Total diode loss

= PDC + PDS

PERS = Output filter capacitor ESR loss

$$= \frac{E_0}{E_0 + E_i}\left(\frac{P_0}{E_0}\right)^2 R_5 + \frac{E_i}{E_0 + E_i}\left[\frac{E_i^2 E_0^2}{12(E_0 + E_i)^2 L_6^2 F^2}\right.$$

$$\left. + \left(\frac{P_0}{eE_i}\,\frac{E_0 + E_i}{E_0} - \frac{P_0}{E_0}\right)^2\right] R_5 \qquad (2.2\text{-}13)$$

POFI = Energy storage inductor core loss

$$= 0.176\,\frac{E_i E_0 Z_6 \sqrt{F}}{(E_i + E_0)N_6} \qquad (2.2\text{-}14)$$

POFC = Energy storage inductor copper loss

$$= \left[\left(\frac{P_0}{eE_i}\,\frac{E_0 + E_i}{E_0}\right)^2 + \frac{E_i^2 E_0^2}{12(E_0 + E_i)^2 L_6^2 F^2}\right] R_6 \qquad (2.2\text{-}15)$$

POF = Total energy storage inductor L_6 magnetic loss

= POFI + POFC

PESC = Input filter capacitor ESR loss

$$= R_4\left[\frac{P_0^2}{E_i E_0 e^2} + \frac{E_i^2 E_0^3}{12(E_0 + E_i)^3 L_6^2 F^2}\right] \qquad (2.2\text{-}16)$$

(2) Parasitic resistance for L_1, L_2, L_6:

The following constraints account for the fact that all core windings contribute some resistance.

$$C(2) = C(3) = C(12) = 0$$

$$C(2) = R_1 A_{C1} - 4\rho F_C N_1 \sqrt{A_1} \qquad (2.2\text{-}17)$$

$$C(3) = R_2 A_{C2} - 4\varphi F_C N_2 \sqrt{A_2} \qquad (2.2\text{-}18)$$

$$C(12) = R_6 A_{C6} - 4\varphi F_C N_6 \sqrt{A_6} \qquad (2.2\text{-}19)$$

(3) Input filter peaking constraint: $C(4) = 0$

This constraint is important in determining the audiosusceptibility performance and the control loop stability.

$$C(4) = C_3^3 + \frac{R_3^2 C_3^3}{L_1} - (PE1)^2 \left\{ C_4^2 + \frac{R_3^2 C_3}{L_1} \left[C_3 - C_4 \left(1 + \frac{L_2}{L_1}\right) \right]^2 \right\} \qquad (2.2\text{-}20)$$

(4) Operating flux density constraint:

This requirement ensures that the magnetic core must not exceed its intended maximum operating flux density. Note that L_6 handles both DC and AC components.

$$C(5) = C(6) = C(9) = 0$$

$$C(5) = \frac{L_1 P_0}{e E_i B_{s1}} - N_1 A_1 \qquad (2.2\text{-}21)$$

$$C(6) = \frac{L_2 P_0}{e E_i B_{s2}} - N_2 A_2 \qquad (2.2\text{-}22)$$

$$C(9) = \frac{L_6}{B_{s6}} \left[\frac{P_0}{e E_i} \frac{E_0 + E_i}{E_0} + \frac{E_i E_0}{2(E_0 + E_i) L_6 F} \right] - N_6 A_6 \qquad (2.2\text{-}23)$$

(5) Window area constraint: $C(7) = C(8) = C(10) = 0$

These constraints ensure that all inductor windings must be accommodated within the physical confines of the available core window area.

$$C(7) = \frac{N_1 A_{C1}}{FW} - \frac{K_1 (Z_1 - \frac{\pi}{2}\sqrt{A_1})^2}{4(K_1 + 1)^2} \tag{2.2-24}$$

$$C(8) = \frac{N_2 A_{C2}}{FW} - \frac{K_2 (Z_2 - \frac{\pi}{2}\sqrt{A_2})^2}{4(K_2 + 1)^2} \tag{2.2-25}$$

$$C(10) = \frac{N_6 A_{C6}}{FW} - \frac{K_6 (Z_6 - \frac{\pi}{2}\sqrt{A_6})^2}{4(K_6 + 1)^2} \tag{2.2-26}$$

(6) Output ripple constraint: $C(11) = 0$

$$C(11) = r - \frac{P_0(E_0 + E_i - eE_i)}{eE_0^2(E_0 + E_i)C_5F} - R_5 \left[\frac{P_0(E_0 + E_i)}{eE_iE_0^2} - \frac{E_i}{2(E_0 + E_i)L_6F} \right] \tag{2.2-27}$$

(7) Frequency dependent source EMI constraints: $C(13) \geq 0$

This constraint limits the maximum percentage of the switching current being reflected back to the source to ensure that the source is not disturbed by the transistor switching action.

$$C(13) = \frac{S}{\sqrt{1\left(\frac{F}{2000}\right)^2}} - \sqrt{A^2 + B^2} \left| H(S) \right|_{max} \tag{2.2-28}$$

$$\text{where} \quad A = \frac{2P_0(E_0 + E_i)}{\pi E_i E_0 e} \quad \text{Sin} \frac{\pi E_0}{E_0 + E_i}$$

$$B = \frac{E_i E_0}{\pi(E_0 + E_i)L_6 F} \left[\cos \frac{\pi E_0}{E_0 + E_i} - \frac{\sin \frac{\pi E_0}{E_0 + E_i}}{\frac{\pi E_0}{E_0 + E_i}} \right]$$

H(S) = Inverse current transfer function of the input filter

2.2.5 Design Constraints for Cuk Converter

The design constraints for the Cuk converter are listed in the same format as that of the conventional Buck-Boost converter. There is a one to one correspondence of the constraints between the two converters.

(1) Loss constraint: C(1) = 0

$$C(1) = P_0(\frac{1}{e} - 1) - PIF - PQ - PD - PESR - POF - PESC$$

where:

PIF = EMI filter copper loss

$$= \left[\frac{P_0}{eE_i}\right]^2 R_{11} + \left[\frac{P_0^2}{e^2 E_i^2} + \frac{E_i^2 E_0^2}{12(E_0 + E_i)^2 L_2^2 F^2}\right] R_{12} \qquad (2.2\text{-}29)$$

PQC = Transistor conduction loss

$$= \frac{P_0 V_{st}(E_0 + eE_i)}{eE_i(E_0 + E_i)} \qquad (2.2\text{-}30)$$

PQS = Turn-on loss + turn-off loss

$$= \frac{T_{sr}F}{6}\left[E_0 + V_d + 2V_{st} + E_i + \frac{P_0}{2(E_0 + E_i)C_4eF}\right]$$

$$\left[\frac{P_0(eE_i + E_0)}{eE_iE_0} - \frac{E_iE_0}{2(E_0 + E_i)F}\left(\frac{1}{L_2} + \frac{1}{L_6}\right)\right]$$

$$+ \frac{T_{sf}F}{6}\left[E_0 + V_d + 2V_{st} + E_i - \frac{P_0}{2(E_0 + E_i)C_4eF}\right]$$

$$\left[\frac{P_0(eE_i + E_0)}{eE_iE_0} + \frac{E_iE_0}{2(E_0 + E_i)F}\left(\frac{1}{L_2} + \frac{1}{L_6}\right)\right] \qquad (2.2\text{-}31)$$

PQB = Base drive loss

$$= \frac{0.1\ P_0V_{be}(E_0 + E_i)}{eE_i(E_0 + eE_i)} \qquad (2.2\text{-}32)$$

PQ = Transistor total power loss

= PQB + PQC + PQS

PDC = Diode conduction loss

$$= \frac{P_0(eE_i + E_0)V_d}{eE_0(E_0 + E_i)} \qquad (2.2\text{-}33)$$

PDS = Diode turn-on loss + turn-off + recovery loss

$$= \frac{T_{nd}F}{12}\left[E_0 + 2V_d - V_{st} + E_i - \frac{P_0}{2(E_0 + E_i)C_4eF}\right]$$

$$\left[\frac{P_0(eE_i + E_0}{eE_iE_0} + \frac{E_iE_0}{2(E_0 + E_i)F}\left(\frac{1}{L_2} + \frac{1}{L_6}\right)\right]$$

$$+\frac{(T_{fd}+3T_{re})}{12}\left[E_0+E_i+2V_d-V_{st}+\frac{P_0}{2(E_0+E_i)C_4eF}\right]$$

$$\left[\frac{P_0(eE_i+E_0)}{eE_iE_0}-\frac{E_iE_0}{2(E_0+E_i)F}\left(\frac{1}{L_2}+\frac{1}{L_6}\right)\right] \qquad (2.2\text{-}34)$$

PD = Diode total loss

= PDC + PDS

PERS = Output filter capacitor ESR loss

$$=\frac{E_i^2E_0^2}{12(E_0+E_i)^2L_6^2F^2}R_5 \qquad (2.2\text{-}35)$$

POFI = Output filter inductor core loss

$$=\frac{0.176\,E_iE_0Z_6\sqrt{F}}{(E_0+E_i)N_6} \qquad (2.2\text{-}36)$$

POFC = Output filter inductor copper loss

$$=\left[\left(\frac{P_0}{E_0}\right)^2+\frac{E_i^2E_0^2}{12(E_0+E_i)^2L_6^2F^2}\right]R_6 \qquad (2.2\text{-}37)$$

POF = Output filter inductor total loss

= POFI + POFC

PESC = ESR loss of energy storage capacitor

$$=R_4\left[\frac{P_0^2}{E_0^2E_i^2}\times\frac{E_ie^2+E_0}{E_0+E_i}+\frac{E_i^2E_0^3}{12(E_0+E_i)^3L_6^2F^2}+\frac{E_i^3E_0^2}{12(E_0+E_i)^3L_2^2F^2}\right] \qquad (2.2\text{-}38)$$

(2) Parasitic resistance for L_1, L_2, L_6:

$$C(2) = C(3) = C(12) = 0$$

$$C(2) = R_1 A_{C1} - 4\rho F_C N_1 \sqrt{A_1} \tag{2.2-39}$$

$$C(3) = R_2 A_{C2} - 4\rho F_C N_2 \sqrt{A_2} \tag{2.2-40}$$

$$C(12) = R_6 A_{C6} - 4\rho F_C N_6 \sqrt{A_6} \tag{2.2-41}$$

(3) Input filter peaking constraint: $C(4) = 0$

This constraint is important in determining the audiosusceptibility performance and the control loop stability.

$$C(4) = C_3^2 + \frac{R_3^2 C_3^3}{L_1} - (PE1)^2 \left(C_4^2 + \frac{R_3^2 C_3}{L_1} \left[C_3 - C_4 \left[1 + \frac{L_2}{L_1} \right] \right]^2 \right) \tag{2.2-42}$$

(4) Operating flux density constraints:

$$C(5) = C(6) = C(9) = 0$$

This constraint ensures that the magnetic core does not exceed its intended maximum operating flux density. Note that both L_2 and L_6 handle DC and AC current.

$$C(5) = \frac{L_1 P_0}{e E_i B_{s1}} - N_1 A_1 \tag{2.2-43}$$

$$C(6) = \frac{L_2}{B_{s2}} \left[\frac{P_0}{e E_i} + \frac{E_i E_0}{2(E_0 + E_i) L_2 F} \right] - N_1 A_1 \tag{2.2-44}$$

$$C(9) = \frac{L_2}{B_{s6}} \left[\frac{P_0}{E_0} + \frac{E_i E_0}{2(E_0 + E_i) L_6 F} \right] - N_6 A_6 \tag{2.2-45}$$

(5) Window area constraints: $C(7) = C(8) = C(10) = 0$

All inductors must be accommodated within the physical confines of the available core window area. All cores are assumed to have the EI configuration.

$$C(7) = \frac{N_1 A_{C1}}{F_W} - \frac{K_1 (Z_1 - \frac{\pi}{2}\sqrt{A_1})^2}{4(K_1 + 1)^2} \tag{2.2-46}$$

$$C(8) = \frac{N_2 A_{C2}}{F_W} - \frac{K_2 (Z_2 - \frac{\pi}{2}\sqrt{A_1})^2}{4(K_2 + 1)^2} \tag{2.2-47}$$

$$C(10) = \frac{N_6 A_{C6}}{F_W} - \frac{K_6 (Z_6 - \frac{\pi}{2}\sqrt{A_6})^2}{4(K_6 + 1)^2} \tag{2.2-48}$$

(6) Output ripple factor constraint: $C(11) = 0$

$$C(11) = r - \frac{E_i}{8(E_0 + E_i)L_6 C_5}\left[\frac{1}{F^2} + \frac{4R_5^2 C_5^2 (E_0 + E_i)^2}{E_i E_0}\right] \tag{2.2-49}$$

(7) Frequency dependent source EMI constraint: $C(13) \geq 0$

This constraint limits the maximum percentage of the switching current being reflected back to the source. The input filter must be designed such that it meets the required attenuation at switching frequency.

Required attenuation at switching frequency

$$= \frac{\text{EMI requirement}}{\text{Fundamental component of switching current}}$$

$$C(13) = \frac{S}{\sqrt{1 + \left(\frac{F}{2000}\right)^2}} - \frac{1}{L_6} \frac{E_0 + E_i}{\pi^2 F} \sin \frac{\pi E_0}{E_0 + E_i} \left|H(S)\right|_{max} \qquad (2.2\text{-}50)$$

where H(S) is the inverse current transfer function of the input filter.

CHAPTER 3

CALCULATION OF THE OPTIMUM CONVERTER DESIGNS

Numerical solution techniques for the nonlinear programming problem (NLP) play an important role in real-world problem solving and decision making. Its applications are found in many unrelated areas, such as, business, engineering, mathematics, social, and physical sciences. In the concrete form, the NLP is that of optimizing (maximizing or minimizing) some physical entity while satisfying some constraints.

The physical entity to be optimized may be power converter weight, profit, cost, efficiency, inventory, energy, etc. In a real world problem because of the limitations of space, funds, physical laws, etc., constraints are often imposed that may limit the possible steps which may be taken to achieve the optimization goals. The transformation of a real world problem into an explicit NLP form through mathematical modeling is an integral part of NLP process. Once an NLP problem is explicitly stated in or modeled by mathematical forms, the task of finding an efficient algorithm to suit the respective application needs becomes a crucial step for a successful implementation of the mathematically formulated NLP.

Most optimization problems arising from practical power converter applications are sufficiently complicated to defy closed-form solutions. Therefore, one has to rely on numerical nonlinear programing algorithms which can provide fast convergence to an optimum

solution from a reasonably good set of initial starting points. When the NLP problem consists of extremizing a function of $\underline{n}$ variables while at the same time requiring these variables to satisfy equality and/or inequality constraints, one has a constrained NLP problem. When the problem is to extremize a function without regard to any constraints, an unconstrained NLP problem results. There are numerous efficient numerical methods for solving the unconstrained NLP problem. In addition, these methods are conceptually simpler and much easier to implement than algorithms that handle the constraints directly. Consequently, algorithms that transform a constrained NLP problem into a sequence of unconstrained NLP problems, such that, the successive solutions of the unconstrained NLP problem converge to the solution of the constrained NLP have been favored in solving the constrained NLP problem. In addition to the ease of extremizing an unconstrained rather than the constrained NLP problem, the effectiveness of the unconstrained NLP algorithms is also an important factor to be considered.

In this chapter, the general theory of transforming a constrained NLP problem to an unconstrained NLP is introduced first. Then the programming aspects of an efficient and effective Nonlinear Programming Technique based on the Augmented Lagrangian Penalty Function Method is elaborated upon to facilitate the comparison and evaluation of the Buck-Boost and Cuk converters.

3.1 Introduction To The Theory of Nonlinear Programming

Stated mathematically, the constrained NLP takes the following form shown as P1, (60):

P1: Minimize Objective Function $f(x)$

Subjective to: Inequality Constraints $p_i(x) \geq 0$

Where $i = 1, 2, 3, \cdots, m_1 < n$

n = dimension of x

Equality Constraints $q_j(x) = 0$

where $j = 1, 2, 3, \cdots, m_2$

where p_i's, q_j's, and f are called the NLP functions which can be linear or nonlinear. For reasons stated previously, this constrained NLP problem is transformed to the unconstrained NLP problem shown as P2 in the following:

P2: Minimize Objective Function $A(\bar{x}, \bar{w}^m, p, q)$, $m = 1, 2, 3, \cdots$

where X = Vector of $\underline{n}$ unknown variables

$A(x, w^m, p, q)$ = New Objective function formed by augmenting the original objective function $f(x)$ with weighted terms (penalty terms) that depend on the constraints p_i, q_j.

$\bar{w}^m$ = Controlling weighting factor, it is a vector of Lagrange Multipliers.

m = Number of iterations.

Based on the transformation to the unconstrained NLP problem, P2, the unconstrained search techniques often incorporate a sequence of unidirectional searches in $\underline{n}$-space, and are based on an iterative scheme

of the following form:

$$x^{k+1} = x^k + \rho r^k, \quad k = \text{iteration number} \qquad (3.1\text{-}1)$$

where a parametric step ρ is taken in a vector direction r^k. The search direction r^k is often decided by the information concerning f and its partial derivatives evaluated both at the point x^k and at previous iteration points. The step ρ is selected to obtain the minimum f(x) in the r^k direction. Also, the influence of constraints imposed on x must be taken into consideration as they alter the way in which the constrained search is chosen. The essence of obtaining the optimum soltuion x through the transformation to unconstrained NLP problems is that of gradually removing the effect of the constraints in the new objective function of a controlled parameter ρ. Using this approach is possible to generate a sequence of unconstrained problems which have solutions converging to a solution of the original constrained problem. Thus, the sequential unconstrained NLP problem consists of finding a sequence of solutions x^m, such that, in the search limit

$$\lim_{m\to\infty} A(x^m, w^m, p, q) - f(x^*) = 0 \qquad (3.1\text{-}2)$$

That is, the iterative guess x^m, of the optimum point approaches the real optimum point x^* as m approaches infinity. In effect, the influence of the constraints on the new augmented objective function $A(x^m, w^m, p, q)$ is relaxed and finally removed in the iteration limit,

and the new augmented objective function, A, converges to the same optimum values $f(x^*)$ of the original objective function.

As an example of a particular method associated with unconstrained P2, consider an augmented function $A(x^m, w^m, p, q)$ defined by including the equality constraints of Courant's quadratic penalty function (55) and the inequality constraints of Carroll's inverse penalty function (56). Define

$$A(x^m, w^m, p, q) = f(x) - w^m \sum_{i=1}^{m_1} P_i^2(x) - \frac{1}{w^m} \sum_{j=1}^{m_2} \frac{1}{q_j(x)} \qquad (3.1\text{-}3)$$

where the last two terms are called the penalty terms. The method generally proceeds as follows. First, select a starting point x^o which is the feasible region associated with inequality constraint (i.e., $q_j(x^o) \geq 0$). Second, design an increasing monotonic sequence $\{w^m\}$ in the program, where

$$\{w^m\} \triangleq \{w^m | w^m > 0,\ w^{m+1} > w^m, \text{ and } w^m \to \infty \text{ as } m \to \infty\} \qquad (3.1\text{-}4)$$

and compute an optimum point x^m, where

$$A(x^m, w^m, p, q) = \min\ A(x, w^m, p, q), \quad m = 1,2,3,\cdots \qquad (3.1\text{-}5)$$

The desired result is that $\lim_{m\to\infty} x^m = x^*$, where x^* is the desired solution to the constrained NLP problem, P1. In the iteration process, it is also well known (57) that

$$\lim w^m \sum_{i=1}^{m_1} P_i^2(x) = 0 \qquad (3.1\text{-}6)$$

That is, the equality constraints are satisfied in the limit. Also in the limit,

$$\lim_{m\to\infty} \frac{1}{w^m} \sum_{j=1}^{m_2} \frac{1}{q_j(x^m)} = 0 \qquad (3.1\text{-}7)$$

That is, the inequality constraints are also satisfied. Thus, $\lim_{m\to\infty} A(x^m, w^m, P, q) = f(x^*)$, the new augmented objective function, converges to the same value as the original objective function at the optimum point x^*.

3.2 Nonlinear Programming Technique Implemented by Using the Augmented Lagrangian (ALAG) Penalty Function Method

The Augmented Lagrangian (ALAG) Penalty Function for the constrained NLP problem, P1, of the previous sections was investigated by Fletcher (58) using the Broyden's Quasi-Newton Method for solving unconstrained nonlinear programming problems. The transformed unconstrained NLP problem given as P3 below.

P3: Minimize $\phi(x, \theta^{(k)}, \sigma^{(k)})$, where

$$\phi(x, \theta^{(k)}, \sigma^{(k)}) = f(x) + \frac{1}{2} \sum_{i=1}^{m_1} \sigma_i^{(k)} \left[P_i - \theta_i^{(k)}\right]^2 + \frac{1}{2} \sum_{j=1}^{m_2} \sigma_i^{(k)} \left[q_i - \theta_i^{(k)}\right]_-^2 \qquad (3.1\text{-}8)$$

and

$$(q_i - \theta_i)_- = \begin{cases} 0, & q_i - \theta_i \geq 0 \\ q_i - \theta_i, & q_i - \theta_i < 0 \end{cases} \qquad (3.1\text{-}9)$$

The algorithms based upon the above transformation approach are

conceptually simple and easy to implement as opposed to the algorithms that handle the constraints directly. The attractive feature of the transformation algorithms is that they take advantage of the existing powerful unconstrained NLP problem which explicitly incorporates the constraint information into the original objective function. Some of the advantages of this method are the ease of programming and the lack of numerical difficulties (59). Other advantages include the fact that algorithms based on this method converge at an ultimately super-linear rate, thus the computational effort per iteration falls off rapidly. Also the initial starting point need not be feasible.

The penalty function transformation technique is sequential in nature since it is essentially an iterative algorithm that requires the solution of an unconstrained NLP problem at each iteration. In addition, the method contains two controlling parameters, α_i and θ_i, whereas, the traditional penalty function includes only one control parameter, such as, the SUMT (Sequential Unconstrained Minimization Techniques) (57). The two controlling parameters are modified and updated to impose an increasing penalty on the penalized objective function as constraint violation increases in order to force the constraint satisfaction.

The theory of nonlinear programming and the Augmented Lagrangian Penalty Function Method presented in the previous sections were applied to the two converters discussed earlier. A flowchart of the general minimization algorithm applied to these converters is

shown in Figure (3.2-1). The steps of this algorithm can be summarized as follows:

(1) At the current search point x^k, generate the search direction r^k.

(2) Find the point $x^{k+1} = x^k + \rho r^k$, which yields the minimum of the augmented function A in the r^k direction from x^k (60).

(3) Calculate and update the status at the new search point x^{k+1}.

(4) Update the Lagrangian Multipliers and controlling parameters for the next iteration.

(5) Test for stopping criteria for every update phase to check stopping conditions in each case, and output termination status if the search is to be finished.

(6) If the stopping criteria is not satisfied, repeat the iterative processes from the new search point x^{k+1}.

The output termination status, the stopping criteria and the effective programming approach will be elaborated upon below.

3.3 Initial Starting Point and Scaling Techniques

The detailed programming aspects of the ALAG will be omitted, only the important information related to the user's applications is presented. The ALAG nonlinear programming package (60) has, in the past few years, gained the recognition as one of the most powerful methods for solving the constrained NLP problem. It is oriented to the user's convenience and ease of programming. The user's programming load is kept to a minimum. It includes one main program and

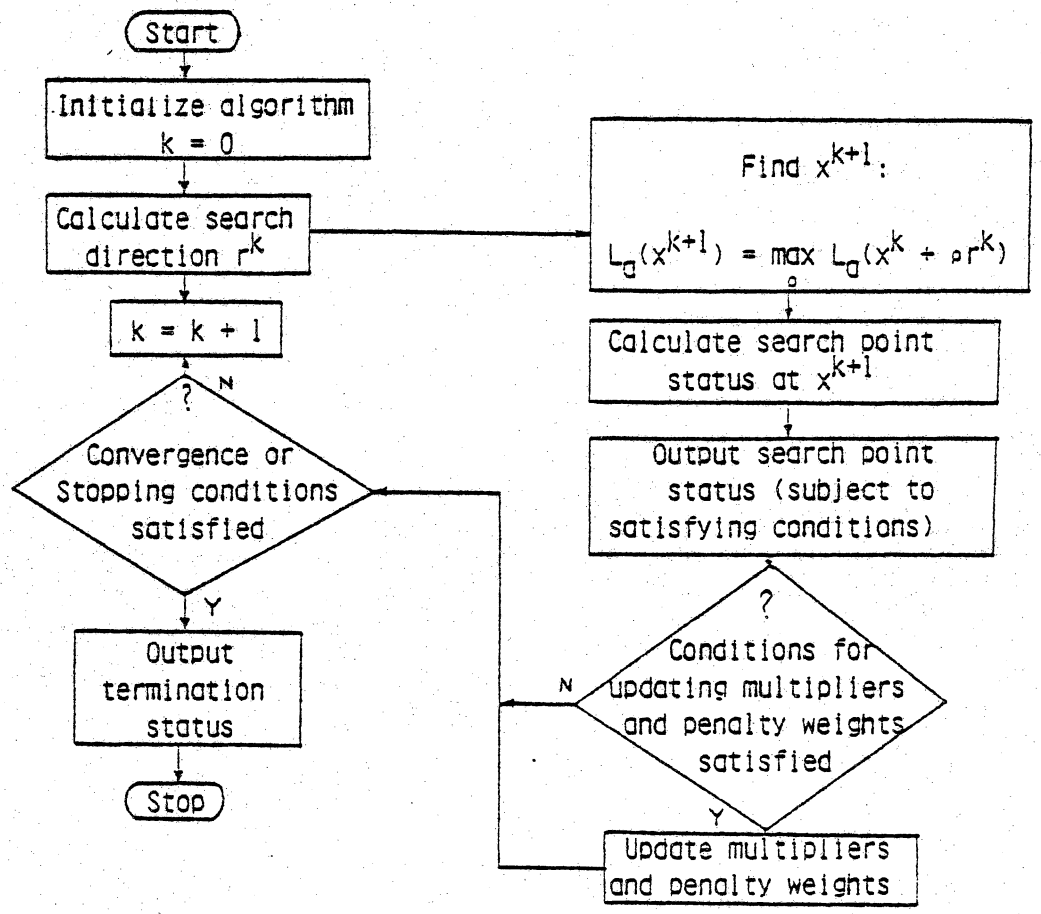

Figure (3.2-1) Flowchart of General Minimization Sequence Using Augmented Lagrangian Multiplier Methods

nine subroutines. The user needs only to supply the main program and one of the subroutines called ALAGB. The main program basically supplies the program controlling parameters, all the input data such as design constants, performance specifications, initial starting point, variable and constraint scaling factors, and the output information with the printing format the user desires. The user-supplied subroutine ALAGB gives the information about objective function, all the equality and inequality constraints and all their first order derivatives which are used to decide the search direction and search step. The important controlling parameters are grouped in the following.

Controlling Parameters:

N: An integer set to the number of variables $N \geq 2$.

M: An integer set to the total number of constraints, $M \geq 1$.

K: An integer set to the total number of equality constraints.

EPS: Variable error tolerance, a real array of N elements for variable stopping criteria. There is one variable tolerance for each variable. In the program, all the tolerances for each variable are set equal.

AKMIN: Constraint error tolerance, a real number which all the scaled constraint residuals must meet in order to satisfy the constraint stopping criteria.

MAXFN: An integer set to the maximum number of calls of the user's subroutine. This is designed to control the computation time in case the program diverges.

3.3.1 Selection of Initial Starting Point

For a complicated nonlinear optimization problem, such as, the switching power converter optimization which has over twenty variables, proper selection of the initial starting point plays an important role on the speed of convergence and accuracy of the solution. The time spent to choose an appropriate initial point prior to running the program is well worth the effort. For each specific practical physical problem, a starting point can usually be obtained based on the designer's past experiences and some simple design equations or design guidelines. As a general rule, the initial starting point should be selected, such that, it satisfies the equality constraints as closely as possible. Meanwhile, it must also satisfy the inequality constraints in order to stay in the feasible region and, therefore, save computation time. A good initial starting point is the first crucial step toward good results and the assurance of a faster rate of convergence. Based on the author's experience, the program has been observed to diverge when a poor initial starting point was chosen.

3.3.2 Variable Scaling Technique and Convergence Tolerance

For a complicated power converter optimization problem, the values of the variables are usually scattered in a wide range. For example, the capacitance may be in the microfarad range and the switching frequency in the hundreds of kilohertz range. These widely scattered variable magnitudes are one of the major causes of slow convergence. Therefore, the variable scaling technique is provided in the program to circumvent this difficulty. It would seem that the

most efficient way of using the variable scaling technique is to choose the variable tolerance EPS around 10^{-4} and then scale all the variables between 1 and 10. For a reasonably acceptable accuracy without using the variable scaling technique, the tolerance EPS is usually set around 10^{-7} for solution accuracy. For the program to exit from computation through variable tolerance stopping criteria, with acceptable accuracy the largest difference between the consecutive iteration of all the variables must be less than the error tolerance. Programming experience indicates that it is easier to control the speed of convergence by using the scaling technique by setting the tolerance around 10^{-4} instead of setting the tolerance around 10^{-7} when not using the inherent scaling feature of the program.

3.3.3 Constraint Scaling Technique and Tolerance

It is very unlikely that the initial starting point can satisfy all the constraints of a complicated NLP problem to the acceptable accuracy within the chosen tolerance. Numerically, the constraint values (or residuals), like the variables, also vary over a wide range. For the power converter optimization, it could extend from 10^{-11} for the simple equality parasitics resistance constraints, through 10^{-1} for the very complicated and lengthy equality loss constraints, to the 10^{2} range for the inequality EMI constraint. Thus, to avoid the situation that certain constraint values are so large as to obscure the effects of the remaining constraints, the constraint scaling technique is also provided to insure that the effect of

violating a given constraint is of the same order of magnitude as that of violating any other constraint.

Faster convergence can be achieved by properly using this scaling technique. Improper use of the scaling technique has been observed to cause the program to diverge. It appears that in this specific application optimization, the program can be brought to a faster rate of convergence by scaling all the constraint values between 10^{-2} to 10^{+2} with the constraint tolerance AKMIN set around 10^{-4}. Whenever the maximum scaled constraint violation $AKK^{(k)}$ is less than the tolerance AKMIN, the stopping criteria is said to be satisfied and the program converges with acceptable accuracy. The above stopping criteria can be better understood by stating it in a more concise mathematical form shown in the following:

$C_i^{(k)}$: Constraint value for ith constraint in iteration k.

SC_i : Scaled factor for the ith constraint.

$WW_i^{(k)}$: The absolute scaled constraint violation for ith constraint in iteration k, that is,

$$WW_i^{(k)} = \frac{|C_i^{(k)}|}{SC_i}$$

$AKK^{(k)}$: Largest scaled constraint violation in iteration k, that is, $AKK^{(k)} = \max_i \{WW_i^{(k)}\}$

Whenever $AKK^{(k)}$ is less than AKMIN in the iteration process, the convergence is said to be reached with acceptable accuracy and computation is terminated.

The program can also be run without the constraint scaling technique. However, for acceptable accuracy the constraint tolerance must be set to less than 10^{-7} instead of 10^{-4}. Based on the author's experience, it is easier to control the speed of convergence by using the scaling technique already built in the program. If the scaled factors are all set equal to one, then the scaling will be rendered inoperable.

3.4 Priority of Computation Stopping Criteria

Satisfaction of the variable and constraint stopping criteria are two of the normal exits of the computer iterations. Another case should be mentioned in the execution process of the program. When the maximum number of calls of the user's subroutine ALAGB is reached, then the program terminates. This maximum number, parameter MAXFN, is preset to limit the computation time in case the program never reaches convergence. The flow chart of the priority of stopping criteria is shown in Figure (3.4-1). The termination of execution through constraint stopping criteria is deemed the most desirable since it satisfies the constraints to the required tolerance. On certain occasions, the exit through satisfying the variable stopping criteria, is accurate enough to be acceptable. The priority of these two normal exits is dependent on how the users choose the variable and constraint tolerances. For example, if the users choose very strict constraint tolerance compared to the variable tolerance, the program will most likely terminate execution through the variable stopping criteria. Depending on how small the tolerance is, the solution may

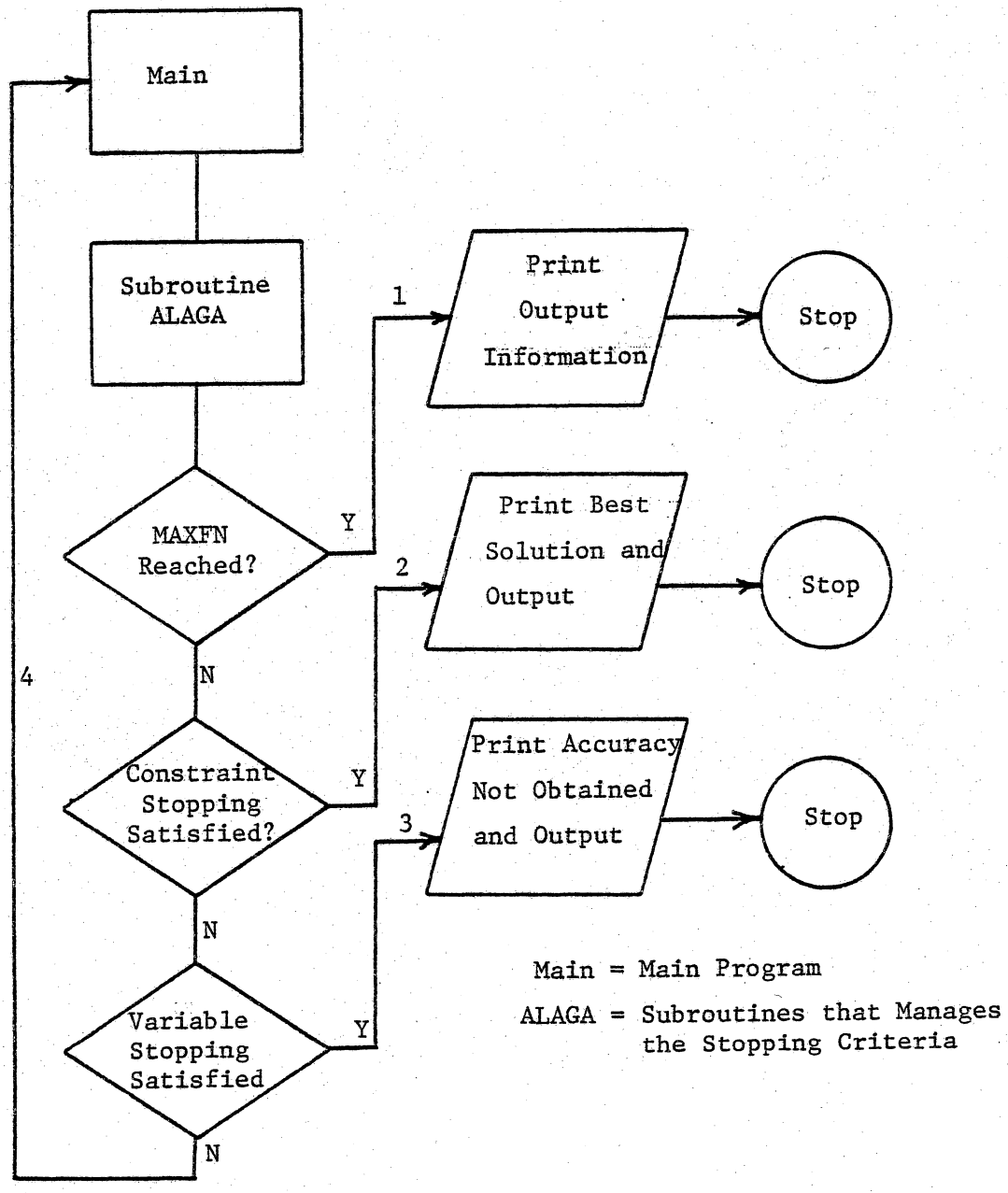

Figure (3.4-1) Flowchart for Priority of Stopping Criteria

be as accurate as the exit from constraint stopping criteria. It is suggested that the users set the constraint tolerance slightly larger (for example, 0.75×10^{-4}) than the variable tolerance (10^{-4}) in order to terminate the execution through the more desirable constraint stopping criteria.

Discussion of Flowchart for Priority of Stopping Criteria

(1) Exit 1

This exit means the objective function has been evaluated the number of times equal to the user's supplied controlling parameter MAXFN. Because the program may still need more executions when reaching MAXFN, the solutions from this exit are in most cases not accurate. The user may increase MAXFN to get proper convergence.

(2) Exit 2

This exit means the largest scaled constraint violation is less than the constraint tolerance. The solution from this exit is considered most desirable.

(3) Exit 3

This exit means the largest difference of all the variables between consecutive iteration is less than the variable tolerance. In this condition, the solution accuracy cannot improve much with more iterations. Depending on the variable tolerance, the solutions through this exit are often acceptable.

(4) Loop 4

If the program does not provide a maximum number of executions of the user's subroutine and if the users do not set a maximum

execution time, then the program continues to circulate in the loop in the event that it is divergent.

3.5 Effective Programming Approaches and Evaluation of the Computer Printouts

The nonlinear programming algorithms based on the Augmented Lagrangian Penalty Function Method is so far the most effective package available in dealing with the NLP problem. However, due to the highly complicated nonlinear constraints and objective function, such as, those encountered in power converter optimization, and due to the complication of the convergence problems, the successful and satisfactory implementation of the NLP is highly dependent on the effective programming techniques. The estimates of the starting point and the utilization of the sacaling technique is crucial in a successful implementation. Based on the author's experience with ALAG, accurate results can be obtained by the efficient and effective approach outlined in the flowchart in Figure (3.5-1). After checking carefully the main program, all the constraints and their respective first order derivatives, the starting point, and the controlling parameters, an effective approach proceeds as follows: (1) use variable and constraint scaling technique as described previously, (2) set computer execution time and printing pages limit in the JCL and run the program, (3) interpret and check the results to see if the results are accurate and acceptable, (4) if yes, perturb the starting point to ascertain whether the results obtained are globally optimum, (5) if the results are not acceptable, check to see if the maximum number of callings of ALAGB have been reached and rerun the program.

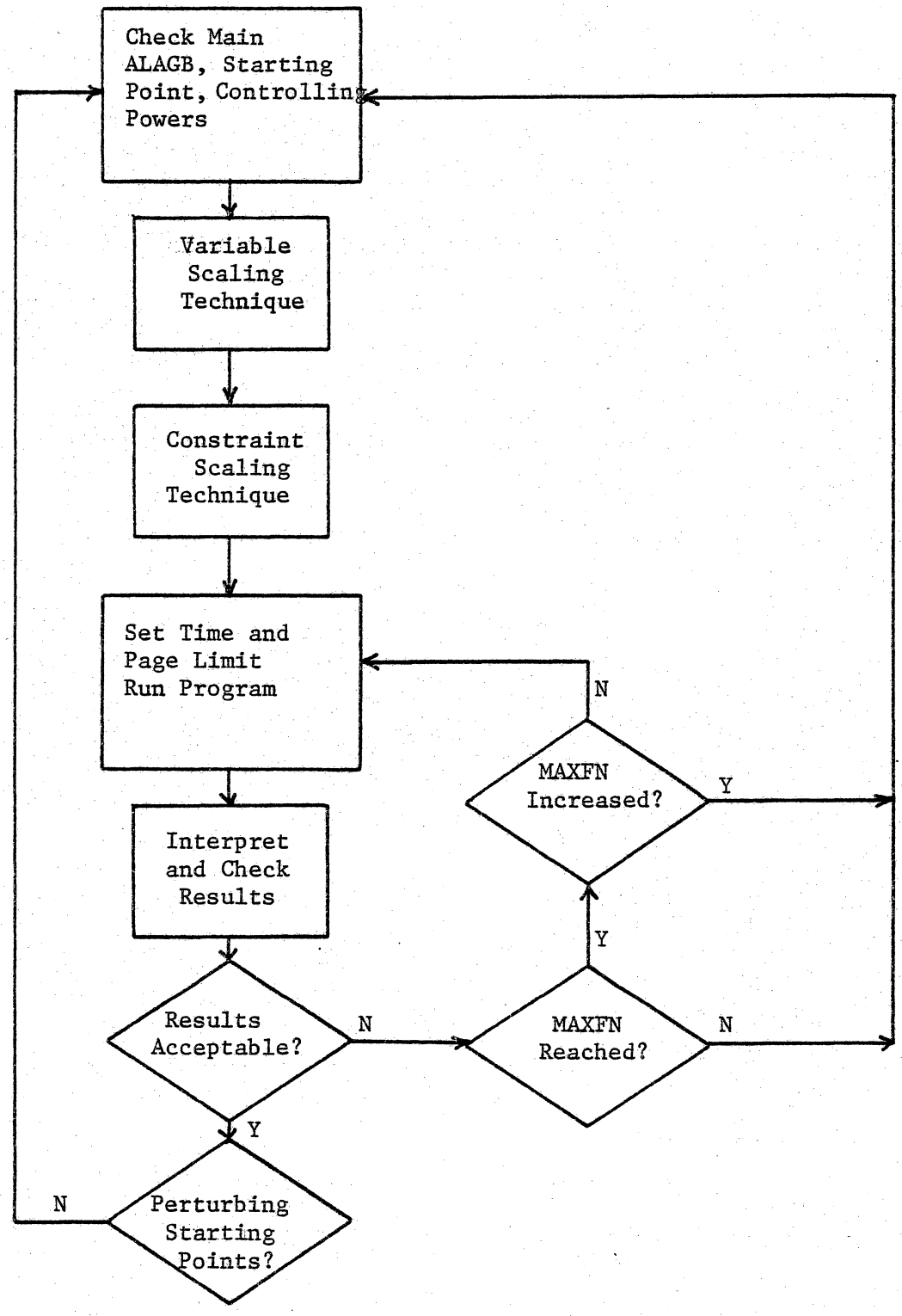

Figure (3.5-1) Flowchart of Effective Programming Approach

Although this process seems laborous and cumbersome, so far it appears to be the best way to run the program in order to obtain better solutions. While interpreting and checking the results, the following evaluation checklist is recommended.

Checklist for the Evaluation of the Outputs

(1) Check whether the solution x stays in the feasible region, that is, whether or not x satisfies the inequality constraints. For equality constraints, the residuals must be within the tolerance; for inequality constraints, what is important is that the inequality is satisfied.

(2) The solution obtained is by the constraint stopping criteria, that is, the largest scaled constraint violation is less than AKMIN.

(3) The solution x is physically reasonable and realizable. The magnetic design, in the case of power converter optimization, should be checked for the realizability due to its complicated design nature.

If the solutions obtained are not acceptable, then it is important to follow the flowchart shown in Figure (3.5-1) and rerun the program.

CHAPTER 4

IMPLEMENTATION AND COMPARISONS OF OPTIMUM CONVENTIONAL BUCK-BOOST AND CUK CONVERTERS

The results of the implementation of the conventional Buck-Boost and Cuk converters obtained through the Nonlinear Programming Technique are presented in this chapter. Detailed comparisons, evaluations, and the implementation of the two converters are made. The coupled-inductor version of the Cuk converter under the balanced and unbalanced current reduction is discussed and compared.

4.1 Basis of Comparisons and List of Symbols

Two comparisons are made between these two converters: (1) Comparison of the loss and weight breakdowns as a function of switching frequency ranging from 20 KHZ to 60 KHZ in 10 KHZ steps; this is the comparison under the constant frequency operation of the optimum design of the two converters for the given frequency; (2) Comparisons of various loss and weight breakdowns under the optimum design; the switching frequency is treated as a variable in the implementation through the nonlinear programming. The bases upon which the comparisons are made are restated in the following with a list of symbols for loss and weight breakdowns.

(1) Basis of Comparisons:

(a) Both converters have the same number of components with different topological connections.

(b) Both perform the same functions of either stepping up or stepping down the input voltage.

(c) Both converters satisfy the same performance requirements and the same design constraints as presented in Chapter 2.

(d) Both converters use the same design constants and the same material, i.e., the same semiconductor and magnetic core materials.

(e) Comparisons are based on the optimum design of both converters. For equitable comparisons, it makes sense to compare the best design of the two converters that satisfy the same performance specifications rather than the comparisons of suboptimum converters given by previous investigators (13).

(2) List of Symbols of Loss and Weight Breakdowns for Comparisons

Loss Breakdowns

PIF = EMI Filter power loss

PQB = Transistor base drive loss

PQS = Transistor switching losses

= Turn-on loss + turn-off loss

PQ = Transistor total loss

= PQB + PQC + PQS

PDC = Diode conduction loss

PDS = Diode switching loss

= Turn-on + Turn-off loss + Recovery loss

PD = Diode total power loss

= PDC + PDS

PQC = Transistor conductor loss

PERS = Output filter capacitor ESR loss

POFI = Energy storage inductor core loss

POFC = Energy storage inductor copper loss

POF = Total loss of energy storage inductor

PMAG = Total magnetic loss

= PIF + POF

PT = Converter total power loss

= PIF + PQ + PD + POF + PERS

Weight Breakdowns

WI = Total magnetic core weight

WW = Total magnetic winding weight

WIW = Magnetic core weight plus winding weight

WS = Source weight

WSM = Source weight contributed by magnetic losses

WH = Packaging weight (including heat sink)

WHM = Packaging weight contributed by magnetic losses

WC = Total capacitor weight

WMAG = Total weight due to magnetics

= WI + WW + WSM + WHM

W = Total converter weight

= WIW + WC + WS + WH

4.2 Implementation and Evaluation of the Optimum Cuk and Conventional Buck-Boost Converters

The numerical values used for the known design constants and performance specifications are presented in Table (4.2-1) and Table

Table (4.2-1)

Numerical Values Used for the Design Constants

F_C:	Window pitch factor (1.9)
F_W:	Core window fill factor (0.4)
ρ:	Conductor resistivity (0.172 x 10^{-7} ohm-m)
D_I:	Core density (7800 Kg/m^3)
D_C:	Conductor density (8900 Kg/m^3)
B_S:	Maximum operating flux density ($B_{S1} = B_{S2} = B_{S6} = 0.4$ W/m^2
D_K:	Weight per farad (D_{k3}, D_{k4}, D_{k5}/210, 1100, 72 kg/F)
V_{ST},V_{BE}:	Voltage drop across collector-emitter and base emitter (0.25, 0.8 volts)
T_{SR},T_{SF}:	Transistor switching times (0.15 μsec, 0.2 μsec)
V_D:	Diode forward voltage drop (0.9 volts)
T_{ND},T_{FD}:	Diode switching times (0.03 μsec, 0.05 μsec. 0.03 μsec)
T_{RE}	
K_H:	Packaging weight density (15.4 Watt/Kg)
K_S:	Source weight density (30.8 Watt/Kg)
K:	Core window area dimensional ratio (1.3)

Table (4.2-2)

Numerical Values Used for the Performance Specifications

P_{El}: EMI filter resonant peaking limit (2)

P_0: Output power (60 Watts)

E_I: Input voltage (15V)

E_0: Output voltage (28V)

S: Frequency dependent source conducted interference (0.1A)

r: Output ripple factor (1%)

(4.2-2). The design constants were obtained through the manufacturer's catalog and data sheets. These known numerical values are used in the computer program to facilitate the comparisons.

4.2.1 Comparisons Under Constant Frequency Operation for the Step-Up Mode

In this subsection, the comparisons are made with the input voltage stepped from 15 volts to 28 volts. The comparisons under the step down mode, that is, input voltage is stepped from 28 volts to 15 volts, will be presented in Section 4.2.3.

By treating the transistor switching frequency as a constant in the computer runs, the loss and weight breakdowns as a function of switching frequency can be obtained. Several advantages are gained using this less complicated but more laborous approach.

(1) By carefully examining the design constraints presented in Chapter 2, it can be found that the transistor switching frequency intertwines from input filter design, through the switching and energy storage/transfer devices, down to the output filter design. Due to this fact and the fact that the constraints are highly nonlinear, it is rather difficult to converge the nonlinear problem. By treating the transistor switching frequency as a constant in each computer run, the convergency difficulty and overwhelming computation time can be alleviated.

(2) Important design insights can be obtained by plotting the detailed weight and loss breakdowns as a function of switching frequency. Instead of identifying a single optimum operating

frequency, the plotted curves will provide perhaps a range of frequency in which the total system weight stays in the minimum value. The optimum operating frequency assessed by this approach (i.e., at the valley point of the plotted curve) can be checked with optimum design by treating the switching frequency as a variable.

(3) The trend and tradeoffs between weight and loss as a function of switching frequency can be readily evaluated and clearly depicted.

The numerically determined loss and weight breakdowns of the conventional Buck-Boost and Cuk converters for the constant frequency mode of operation are plotted in Figures (4.2-1) and (4.2-2) respectively. The symbol B in the parenthesis stands for the conventional Buck-Boost converter and the C stands for the Cuk converter. The magnetic components, such as inductors and transformers, constitute one of the major ingredients of a switching power processing system. Their impact on the total converter system loss and weight breakdowns as a function of switching frequency are also plotted in Figure (4.2-3) and Figure (4.2-4) respectively.

Discussion:

(1) By comparing the total losses and loss breakdowns of the two converters as shown in Figure (4.2-1), it can be seen that the conventional Buck-Boost converter is inferior to the Cuk converter in each respect. This points out that the Cuk converter

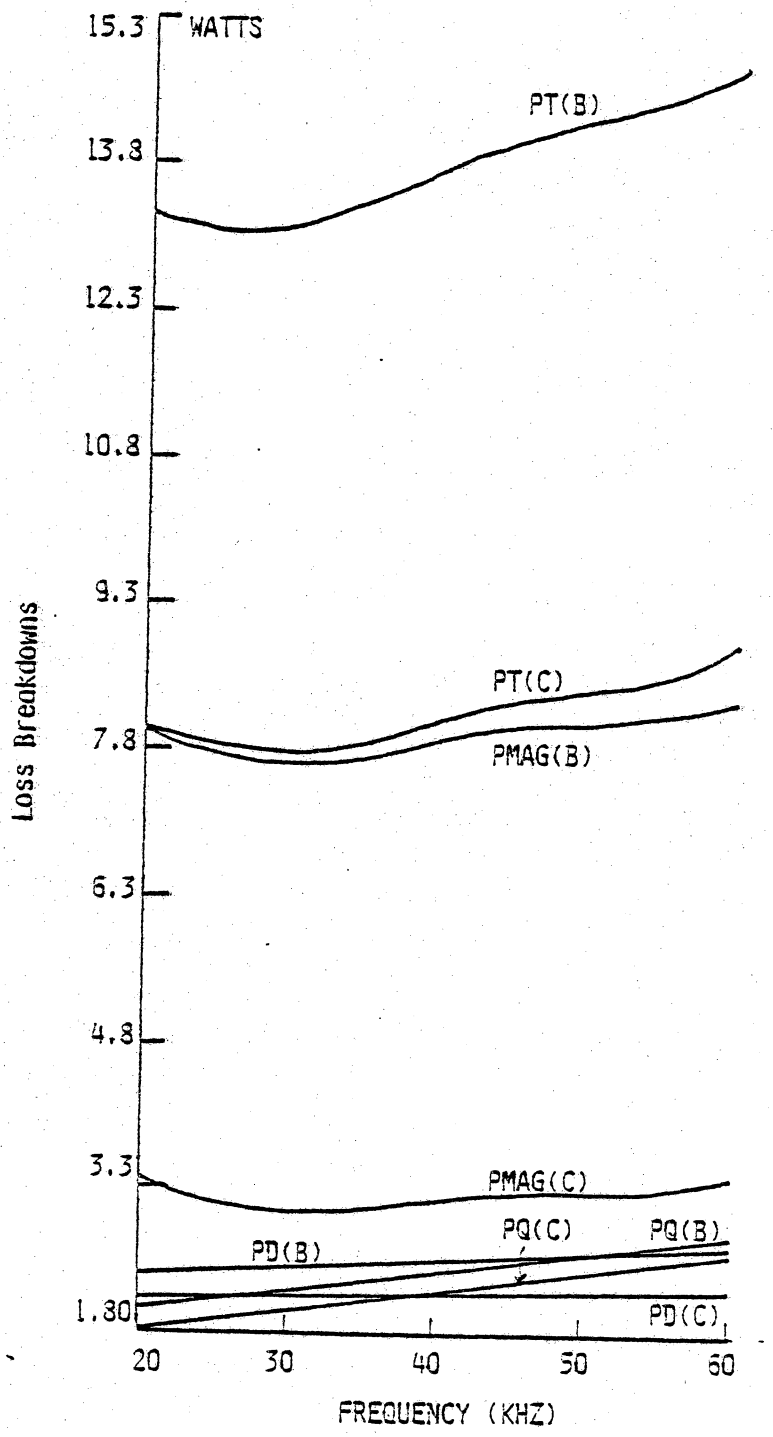

Figure (4.2-1) Loss Breakdowns for the Two Converters at Constant Frequency Operation Under the Step-Up Mode

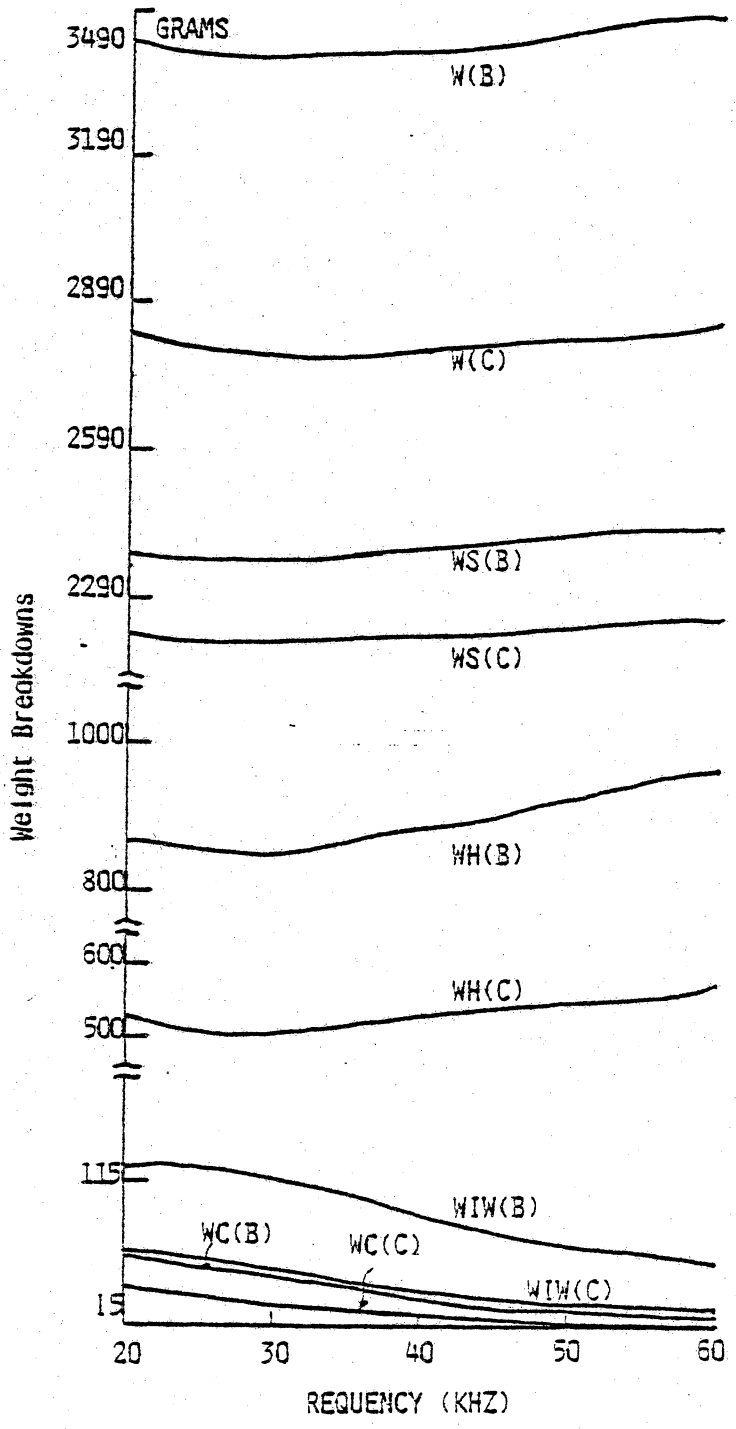

Figure (4.2-2) Weight Breakdowns for the Two Converters at Constant Frequency Operation Under the Step-Up Mode

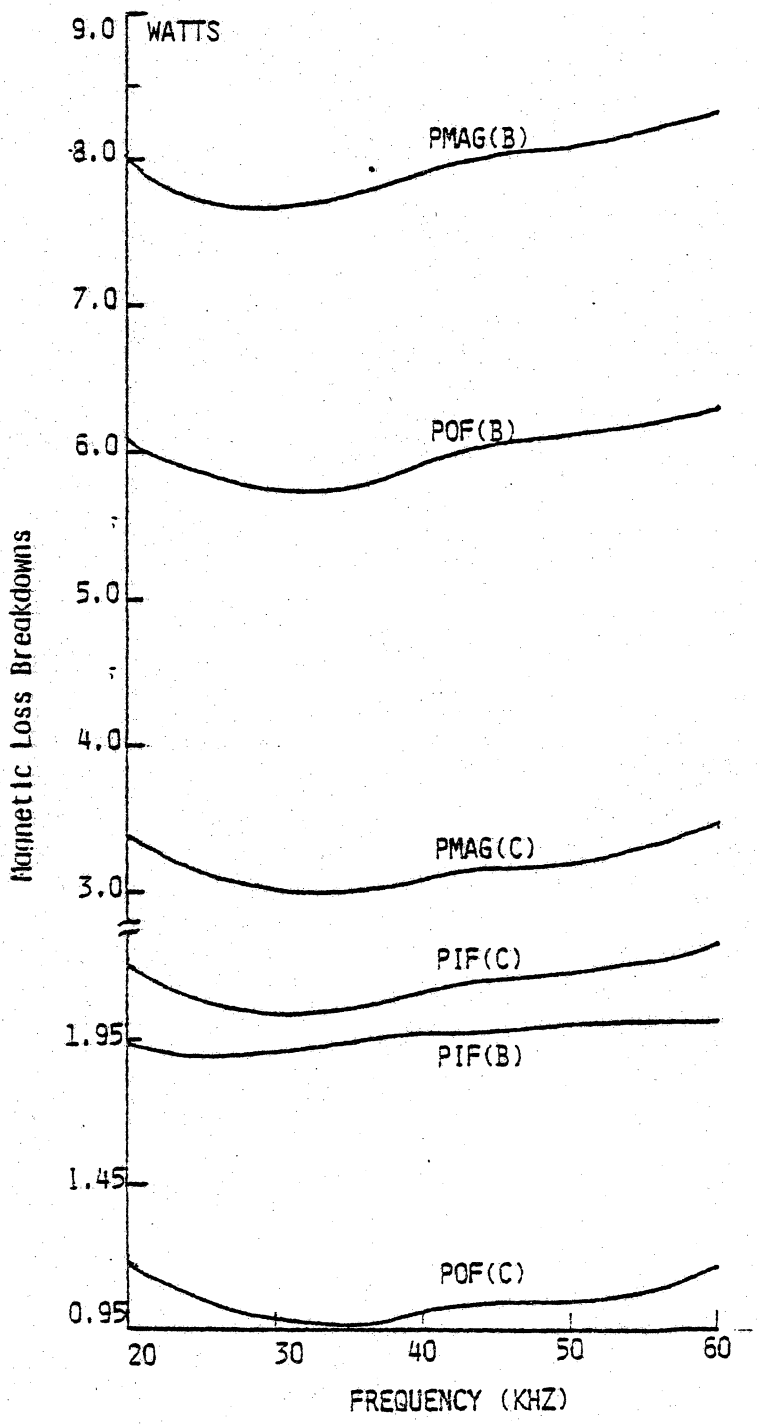

Figure (4.2-3) Magnetic Loss Breakdown at Constant Frequency Operation under the Step-Up Mode

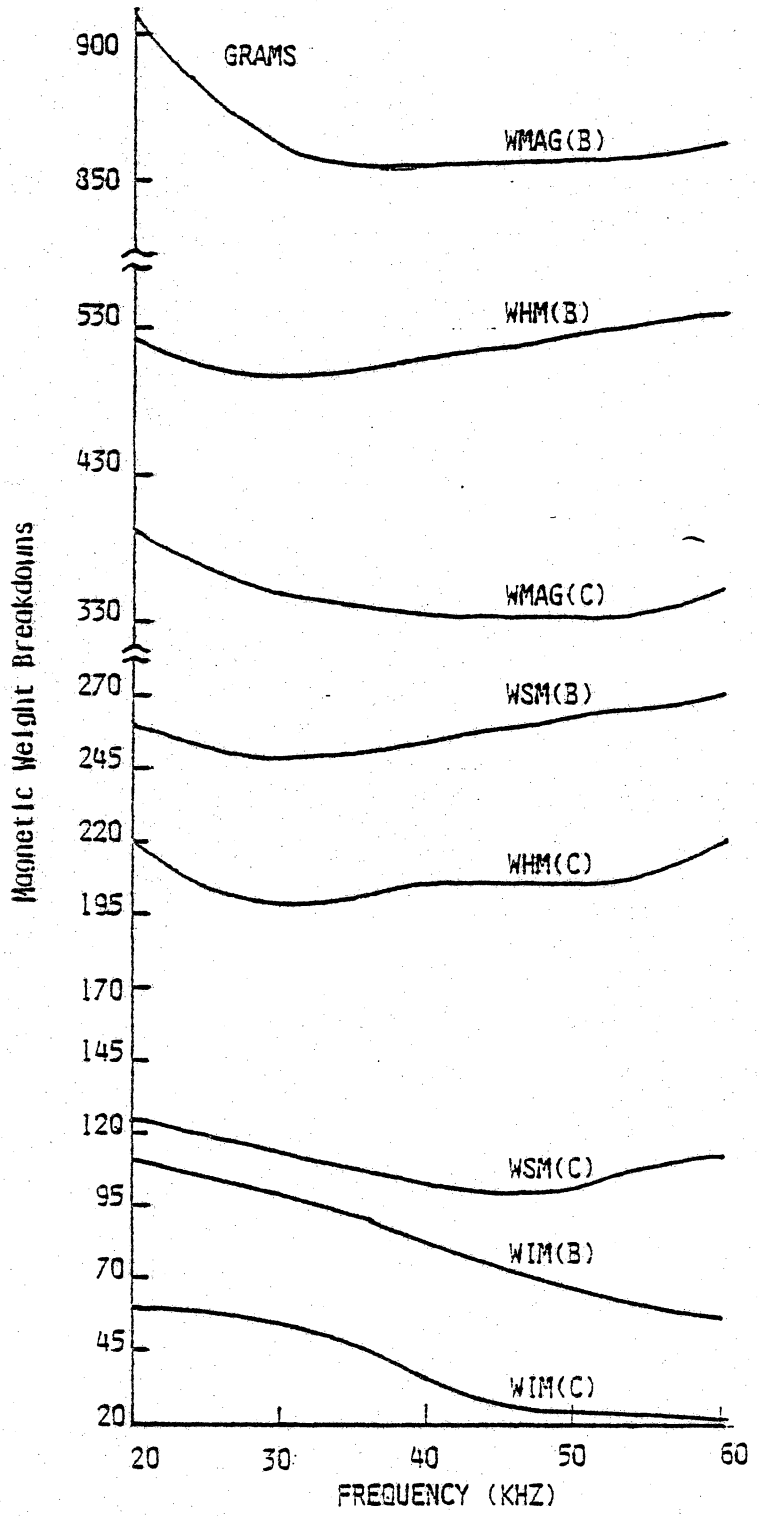

Figure (4.2-4) Magnetic Weight Breakdowns at Constant Frequency Operation under the Step-Up Mode

is more efficient in supplying the same DC output power for the same performance specifications and constraints.

(2) The total loss is observed to have a U-shape curve for both converters. The decrease of the total loss at lower switching frequencies is caused by the reduction of the winding copper losses of the magnetic components, the rapidly increasing total loss at the higher frequency end is caused by the rapidly increasing semiconductor switching losses. Due to the interaction of these two effects at low and high frequency ends, the U-shape is thus formed.

(3) One of the advantages of operating the switching power converter at as high a frequency as possible is the reduction of magnetic size and weight with frequency as shown in Figure (4.2-2) for curve WIW. As a result of the rapidly increasing total loss at the high frequency end, the source and heat sink weight increase; thus the advantageous weight reduction due to the shrinking magnetic components is much more than counterbalanced. This U-shape effect as observed in Figure (4.2-1) and Figure (4.2-2) sets the maximum switching frequency for an efficient switching power converter operation (i.e., either minimum weight or minimum loss). This observation points out an important fact that for each specific application of a switching power converter, there must be an optimum operating frequency to achieve the objective of the minimum loss or minimum weight operation. Iterative design processes by randomly selecting a switching

frequency, turn out to be very time-consuming and result in a suboptimum design. This subjective brute-force, trial-and-error process should be avoided now that an efficient Nonlinear Programming Technique is available.

(4) In order to see the impact of magnetics on the operation of a switching power converter more clearly, the information of the related magnetic loss and weight breakdowns is extracted and plotted in Figures (4.2-3) and (4.2-4). The decreasing magnetic size and weight are depicted clearly as a function of increasing switching frequency shown as curve WIM. There is, however, a practical limit on the maximum operating frequency due to the increasing source and packaging weight contributed by the increasing total magnetic losses shown as PMAG in Figure (4.2-3). Also, shown in Figures (4.2-3) and (4.2-4) are the magnetic loss and weight breakdowns of the two converters. The Cuk converter is clearly superior to the conventional Buck-Boost converter in every loss category.

(5) The weight breakdowns as a function of switching frequency only point out a frequency range for optimum operation. The optimum operating frequency can be pinpointed in one attempt by treating the switching frequency as a variable in the computer implementation as presented in the following subsection. The results obtained for constant frequency and variable frequency operations can be compared with each other as will also be presented in the next section.

4.2.2 Comparisons of the Optimum Designs at the Optimum Frequencies for the Step Up Mode

By examining the design constraints in Chapter 2 carefully, the switching frequency can be found in many of the complicated non-linear constraints, such as, the loss constraint, output ripple factor constraint, and EMI constraint, etc. Due to the intertwining of the switching frequency from the input filter down to the output, it is rather difficult to get the program to converge in a short computation time. However, there is one advantage of treating the switching frequency as a variable. Instead of locating a range of suitable switching frequencies and components, the overall design information can be pinpointed in just one attempt.

Instead of plotting the loss and weight breakdowns as a function of switching frequency, the computing results of the two converters are tabulated in Tables (4.2-3) and (4.2-4) for comparison. Also, by reading the curves of weight breakdowns as shown in Figure (4.2-2) obtained through constant frequency operation, the optimum operation of the two converters fall in the range between 30 KHZ and 40 KHZ. In order to double check that the results through the computer implementation by treating the frequency as a variable fall in the valley of the curves obtained by plotting the loss and weight breakdowns against frequency, the computer results of 30 KHZ, optimum design and 40 KHZ for both converters are tabulated in Tables (4.2-5) and (4.2-6) for loss and weight breakdowns to make sure that the results coming from both operations are consistent.

Table (4.2-3)

Comparison of Loss Breakdowns for Both Converters for the Optimum Design under the Step Up Mode

		Cuk	Buck-Boost
F		39,276 HZ	34,473 HZ
Unit		Watts	Watts
Input Filter Loss	PIF	2.1299	1.9095
Transistor Losses	PQB	0.3461	0.3856
	PQC	1.0815	1.2049
	PQS	0.7446	0.6804
	PQ	2.1722	2.2709
Diode Losses	PDC	2.0858	2.3237
	PDS	0.0887	0.1394
	PD	2.1745	2.4631
ESR Loss	PERS	0.0483	0.2165
Output Filter Losses	POFC	0.8878	5.3007
	POFI	0.1459	0.4215
	POF	1.0338	5.7222
Magnetic Loss	PMAG	3.1637	7.6317
Total Loss	PT	7.5587	12.5822
Efficiency	e	0.8887	0.8299

Table (4.2-4)

Comparison of Weight Breakdowns for Both Converters for the Optimum Designs Under the Step-Up Mode

F	39,276 HZ	34,473 HZ
Unit	Grams	Grams
WI	17.6	55.5
WW	16.1	55.2
WIW	33.7	110.7
WSM	102.7	247.8
WS	2191.9	2347.2
WHM	205.4	495.6
WH	487.8	798.3
WC	20.7	47.1
WMAG	341.8	854.1
W	2734.1	3303.3

Discussion:

By examining the loss and weight breakdowns of the optimum designs of both converters shown in Tables (4.2-3) and (4.2-4) the following observations can be made:

(1) The Cuk converter outperforms the conventional Buck-Boost converter from both the efficiency and weight point of views. A total of 73 watts of input power are required for Buck-Boost converter to supply the required 60 watts output due to its lower efficiency operation. The Cuk converter on the other hand requires only 68 watts at the input which accounts for its almost 90% power conversion efficiency.

(2) By comparing the detailed loss and weight breakdowns of both converters item by item, the Cuk converter demonstrates better performance, thus culminating in an overall better performance. One striking difference between the detailed comparison shows that the magnetic losses of the energy storage inductor of the conventional Buck-Boost converter contributes a major loss (almost 45% of total losses); this loss is mainly from the copper loss of the energy storage/transfer inductor since a large current passes through this device. This large current is caused by the topological position of the transistor and diode which interconnect the input and output ports. These two switching devices disconnect the input and output ports during the entire switching cycle. This produces a large current pulse through the switching devices and results in a load-dependent output voltage ripple. In the Cuk converter, on the other hand, the energy storage/transfer capacitor always

interconnects the input and output ports during the entire switching cycle. Due to the topological differences between the two converters, large differences in performance result for the same voltage conversion function.

(3) The detailed loss breakdowns show that the DC conduction losses of the switching devices contribute the major portion to the total transistor and diode losses. This is only true for the low frequency end around 40 KHZ or below. The fact is that the device switching losses increase rapidly at the high frequency end over 100 KHZ, and become the dominant factor of the total device losses. Due to the rapidly increasing switching losses, with frequency at the high frequency end, high speed switching devices become a vital factor for high frequency switching power converters. This is necessary in order to take advantage of the decreasing size and weight of the magnetic and capacitive components with increasing frequency (61).

(4) In order to show that the data obtained by treating the frequency as a variable yields an optimum design, the results of the 30 and 40 KHZ obtained from constant frequency operation are tabulated with that of the variable frequency operation in Tables (4.2-5) and (4.2-6). The consistency and continuity of these three results demonstrate that the optimum design obtained through variable frequency operation is reasonably accurate. However, one fact needs to be brought out at this point, that the minimum weight design of the power converter does not necessarily imply the achievement of the minimum loss at the same operating point.

Table (4.2-5)

Comparison of Loss and Weight Breakdowns of the Buck-Boost Converter for 30 KHZ, 34.5 KHZ (optimum) and 40 KHZ Operation

Loss	30 KHZ	Optimum (34,473 HZ)	40 KHZ
Unit	Watts	Watts	Watts
PQ	2.1906	2.2709	2.4038
PD	2.4483	2.4631	2.5156
PERS	0.1909	0.2165	0.2509
PMAG	7.6616	7.6317	7.9105
PT	12.4915	12.5822	13.0808
Weight	**Kg**	**Kg**	**Kg**
WI	0.0581	0.0555	0.0433
WW	0.0576	0.0552	0.0389
WS	2.3531	2.3472	2.3731
WH	0.8100	0.7983	0.8501
WC	0.0503	0.0471	0.0355
WMAG	0.8620	0.8541	0.8527
W	3.3292	3.3034	3.3409

Table (4.2-6)

Comparison of Loss and Weight Breakdowns of the Cuk Converter for 30 KHZ, 39.3 KHZ (Optimum) and 40 KHZ Operation

Loss	30 KHZ	Optimum (39,276 HZ)	40 KHZ
Unit	Watts	Watts	Watts
PQ	1.9853	2.1722	2.1855
PD	2.1515	2.1745	2.1797
PERS	0.0455	0.0483	0.0523
PMAG	3.0331	3.1637	3.1580
PT	7.2163	7.5587	7.5754

Weight	Kg	Kg	Kg
WI	0.0290	0.0176	0.0178
WW	0.0254	0.0161	0.0162
WS	2.1820	2.1919	2.1940
WH	0.4679	0.4878	0.4919
WC	0.0326	0.0207	0.0203
WMAG	0.3498	0.3418	0.3416
W	2.7370	2.7341	2.7403

This point is brought out by the fact that the total loss of the minimum weight design at 39,276 HZ and 34,473 HZ for Cuk and Buck-Boost converters respectively are higher than those at the 30 KHZ operation. This fact again manifests the tradeoff between loss and weight of a switching power converter as the switching frequency is increased.

In order to show the percentage contribution of the loss and weight breakdowns of both converters, Tables (4.2-7) and (4.2-8) are provided. Some discussion based on these data follows.

(5) Device switching losses account for a substantial portion of the total losses for both converters. Another major contribution of the loss comes from the magnetic copper and core loss. These two major losses set the limit of the maximum operating frequency.

(6) Magnetic weight contributes a substantial part, therefore, improper design could cause the loss and weight penalty to increase. However, the largest portion of weight comes from the output power requirement. Higher output power requires heavier total weight.

(7) Capacitor weight contributes a minor portion to the overall converter weight and at the same time does not involve the complicated factors as found in the design of magnetic components.

(8) The device stresses include the voltage and current ratings. The current stress is measured when the device is in conduction. The voltage stress is measured when the device is cut off. The

Table (4.2-7)

Percentage Comparisons of Power Losses of Both Converters for the Optimum Designs of the Step-Up Mode

	Cuk 39,276 HZ		Buck-Boost 34,473 HZ	
Unit	%	(Watts)	%	(Watts)
Input Filter Loss	28.18	(2.1299)	15.18	(1.9095)
Transistor Loss	28.74	(2.1722)	18.05	(2.2709)
Diode Loss	28.76	(2.1745)	19.58	(2.4631)
ESR Loss	0.64	(0.0483)	1.72	(0.2165)
Output Filter Loss	13.68	(1.0338)	45.47	(5.7222)
	100	(7.5587)	100%	(12.5822)

Table (4.2-8)

Percentage Comparisons of Weight Breakdowns of Both Converters for the Optimum Designs of the Step-Up Mode

Frequency	Cuk 39,276 HZ		Buck-Boost 34,473 HZ	
Unit	%	(g)	%	(g)
Weight from Magnetics	12.48	(341.85)	25.64	(854.08)
Weight from Capacitors	0.92	(25.40)	2.05	(68.19)
Weight from Switching Losses	15.46	(423.38)	13.84	(460.87)
Weight for Power Output Requirement	71.13	(1948.05)	58.47	(1947.85)
	99.99%	(2738.68)	100%	(3330.99)

comparison of the device stresses of both converters are shown in Table (4.2-9). In this table, the device forward voltage drop and the small switching ripple are neglected. From this table, the voltage stress of the transistor and diode of both converters are equal. The average current stress of the Buck-Boost converter is slightly higher than that of the Cuk converter since there is an efficiency factor $(E_0 + eE_i)$ involved in the numerator of the Cuk converter compared to that of $(E_0 + E_i)$ for the Buck-Boost converter as shown in the Table, and the efficiency e is always less than one. Because $\frac{E_0}{D} = \frac{E_i}{1-D}$ (this is the input-output voltage relationship for the two converters, the original equation is $\frac{E_0}{E_i} = \frac{D}{1-D}$), so the voltage stress of the two converters are equal as also shown in Table (4.2-9).

4.2.3 Comparisons of Cuk and Buck-Boost Converters in the Step Down Mode

Since both the Cuk converter and the conventional Buck-Boost converter can either step up or step down the input voltage, the voltage step down case is investigated in this subsection in order to complete the evaluation and comparison. The loss and weight breakdowns for both converters when the input voltage is stepped from 28 volts down to 15 volts are tablulated in Tables (4.2-10) and (4.2-11) respectively.

Discussion:

Tables (4.2-10) and (4.2-11) are obtained by swapping the input and output voltage of the previous two subsections with the

Table (4.2-9)

Comparison of Device Stresses of the Buck-Boost and Cuk Converters

	Cuk	Buck-Boost
Transistor Voltage Stress	$\frac{E_0}{D}$	$\frac{E_i}{1-D}$
Diode Voltage Stress	$\frac{E_0}{D}$	$\frac{E_i}{1-D}$
Transistor Average Current	$\frac{P_0(E_0+eE_i)}{eE_iE_0}$	$\frac{P_0(E_0+E_i)}{eE_iE_0}$
Diode Average Current	$\frac{P_0(E_0+eE_i)}{eE_iE_0}$	$\frac{P_0(E_0+E_i)}{eE_iE_0}$

Table (4.2-10)

Comparison of Loss Breakdowns for Both Converters When the Input Voltage is Stepped Down from 28V to 15V

	Cuk	Buck-Boost
F	44,830 HZ	36,488 HZ
Unit	Watts	Watts
Input Filter Loss	1.009	0.4041
Transistor Losses	1.6424	1.5532
Diode Losses	3.8149	4.4298
ESR Loss	0.0289	0.1077
Output Filter Losses	2.7486	5.0724
Magnetic Losses	3.7576	5.4764
Total Loss	9.2439	11.5672
Efficiency	0.8669	0.8403

Table (4.2-11)

Comparison of Weight Breakdowns for Both Converters
When the Input Voltage is Stepped Down from 28V to 15V

	Cuk	Buck-Boost
F	44.830 HZ	36.488 HZ
Unit	Kg	Kg
Core and Winding Weight	0.0163	0.0777
Source Weight	2.2472	2.3184
Packaging Weight	0.5983	0.7406
Capacitor Weight	0.1196	0.0471
Magnetic Total Weight	0.3823	0.6112
Total Weight	2.9815	3.1839

rest of design constants and performance requirements not changed.

(1) The Cuk converter is again superior to the Buck-Boost converter in both the loss and weight breakdowns.

(2) When compared with the previous voltage step-up case given in Tables (4.2-3) and (4.2-4), the Cuk converter gets worse because higher losses and heavier weights due to the larger current flowing in the output port resulting from the smaller output voltage (from 28 volts in the step-up case to the 15 volts in the present step-down case. This results in higher winding copper losses in the output filter inductor. The copper loss of the Buck-Boost converter, on the other hand, decreases because the increase input voltage decreases the current passing through the magnetic component, which results in lower magnetic losses.

(3) The optimum operating frequency of the Cuk converter increases from 39,276 HZ to 44,830 HZ, and for the Buck-Boost converter, it increases from 34,473 HZ to 36,488 HZ. This information shows that in order to obtain the optimum design, both converters must operate at higher frequencies for the step-down case.

4.3 Evaluation of the Optimum Coupled Inductor Cuk Converter for Balanced and Unbalanced Current Reduction

The coupled inductor version of the Cuk converter is shown in Figure (4.3-1a). The 1:1 proportionality of the two inductor voltage waveforms shown in Figure (4.3-1b) has led to the idea of coupling the inductors together (14,19). This inductive coupling does

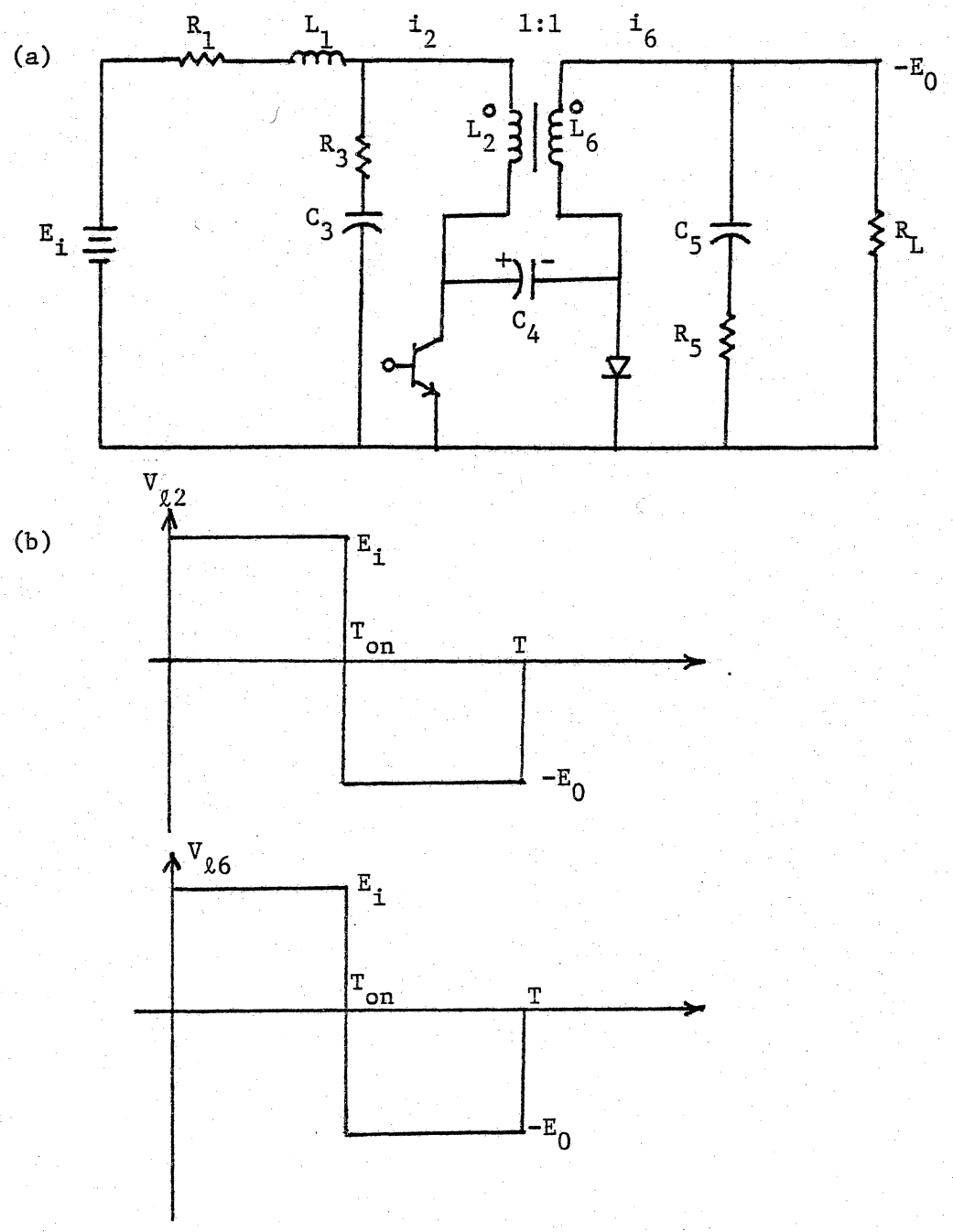

Figure (4.3-1) The Coupled Inductor Version of Cuk Converter

(a) Circuit Configuration

(b) Proportional Voltage Waveforms Across the Coupled Inductor

not alter the basic DC to DC conversion property. However, the coupling of these inductors allows a reduction in both the input and output current ripples. Thus, in addition to the capacitive energy transfer through the electric field, there is now an additional energy transfer through the magnetic field and the inductive coupling. Depending upon the relationship between the coupling coefficient k and the effective turns ratio n, the current ripples can be steered to either side of the coupled inductor (14,19). These two parameters are defined as follows:

$$k = \frac{L_m}{\sqrt{L_{22}L_{66}}} \tag{4.3-1}$$

$$n = \frac{L_{22}}{L_{66}} \tag{4.3-2}$$

where L_m is the mutual inductance, L_{22} and L_{66} are the self-inductances of primary and secondary windings. Two cases of current ripple reduction are discussed in the following.

(1) Balanced reduction of current ripples

In this case, n = 1, and the current ripples are reduced equally as shown in the following.

$$\frac{d_{i2}}{dt} = \frac{d_{i6}}{dt} = \frac{V_{\ell 2}}{(k+1)L_{22}} = \frac{V_{\ell 6}}{(k+1)L_{66}} \tag{4.3-3}$$

As seen from the above equation, in the limit as the coupling coefficient k approaches are (tight coupling), both the current ripples are reduced by two. This means the effective primary and secondary inductances are doubled by tight coupling.

(2) Unbalanced reduction of current ripples

In this case $n \neq 1$ and $k < n < \frac{1}{k}$ (14,19). The effective primary and secondary inductances L_{efp} and L_{efs} are shown in the following.

$$L_{efp} = L_{22}(1 + k)\ \frac{1 - k}{1 - kn} \qquad (4.3\text{-}4)$$

$$L_{efs} = L_{66}(1 + k)\ \frac{1 - k}{n - k}\ n \qquad (4.3\text{-}5)$$

The following values are chosen for n and k.

$$n = 0.996 \quad \text{and} \quad k = 0.995$$

These result in effective inductances of

$$L_{efp} = \frac{10}{9} L_{22} \quad \text{and} \quad L_{efs} = 10\ L_{66}$$

These two cases are implemented using the nonlinear programming package to investigate the merits of the coupled inductor version of Cuk converter for both the balanced and unbalanced reduction of current ripple. The calculated loss and weight breakdowns of the optimum designs for these two cases are tabulated in Tables (4.3-1) and (4.3-2) for comparison and evaluation.

Table (4.3-1)

Comparisons of Power Losses of Coupled Inductor Cuk Converter for the Balanced and Unbalanced Current Ripple Reduction Modes

Unit	Unbalanced Reduction Watts	Balanced Reduction Watts
Input Filter Loss	2.1629	2.2024
Device Switching Losses	4.3283	4.3394
ESR Loss	0.0187	0.1053
Output Filter Copper Loss	0.1702	0.3771
Output Filter Core Loss	0.4477	0.4659
Total Magnetic Loss	2.7807	3.0455
Total Converter Loss	7.1278	7.4902

Table (4.3-2)

Comparison of Weight Breakdowns of the Coupled Inductor Cuk Converter for the Balanced and Unbalanced Current Ripple Reduction Modes

	Unbalanced Reduction	Balanced Reduction
Unit	Kg	Kg
Core Weight	0.0132	0.0186
Winding Weight	0.0194	0.0223
Source Weight	2.1789	2.1878
Packaging Weight	0.4616	0.4795
Capacitor Weight	0.0123	0.0255
Total Magnetic Weight	0.3035	0.3375
Total Converter Weight	2.6854	2.7337

Discussion of the Results:

(1) As expected, it is more advantageous to operate the coupled inductor version of the Cuk converter under the unbalanced current ripple reduction. Depending on whether the EMI requirement or the output ripple factor is more desirable, the ripple can be steered to the input or output side. Also, the total magnetic weight of the unbalanced reduction case is less than that of the balanced reduction case. There is approximately a 50 gram reduction in the total weight under the unbalanced case from that of the balanced case.

(2) It is interesting to compare the output filter ESR loss and the output filter inductor copper loss for the two cases. Inspection of Table (4.3-1) reveals that these two loss factors are noticeably different while all the other loss factors are only slightly different. This comparison supports the fact that the effective secondary inductance is ten times the self inductance before the coupling for the unbalanced case, thus the current ripple is steered to the input side resulting in lower losses in the output filter inductor and capacitor. The simulation results presented in these tables are in agreement with what theory predicts. Due to the reduction of the output filter loss for the unbalanced current reduction, the total loss is also smaller in this case.

4.4 Profiles of the General Characteristics for the Buck-Boost and Cuk Converter

The magnetic and capacitive component values obtained by treating the frequency as a constant ranging from 20 KHZ to 60 KHZ in 10 KHZ steps are shown in Tables (4.4-1) and (4.4-2) for the Buck-Boost and Cuk converters. These two tables give the general trend of the magnetic and capacitive sizes as the switching frequency is increased. Also, Figures (4.2-1) to (4.2-4) describe the general trend of the loss/weight breakdowns as the switching frequency is increased. By examining tables and figures, profiles of the general characteristics of the loss/weight breakdowns and the magnetic/capacitive components as a function of the switching frequency can be summarized as follows:

(1) Profiles of Loss Breakdowns

(a) Quantities that have a U-shape curve are listed in the following:

1. Total loss
2. Total magnetic loss
3. Winding copper loss

(b) Quantities that increase with frequency:

1. Transistor total losses
2. Diode total losses
3. Magnetic core loss

(2) Profiles of Weight Breakdowns

(a) Quantities that have a U-shape curve:

1. Total converter weight

Table (4.4-1)

Component Design Values of Buck-Boost as a Function of Frequency

	20 KHZ	30 KHZ	40 KHZ	50 KHZ	60 KHZ	Unit
A_1 ($\times 10^{-4}$)	0.533	0.531	0.408	0.341	0.291	m^2
A_{C1} ($\times 10^{-6}$)	1.30	0.25	0.912	0.783	0.691	m^2
Z_1 ($\times 10^{-1}$)	0.677	0.659	0.546	0.493	0.456	m
L_1 ($\times 10^{-3}$)	0.269	0.256	0.179	0.141	0.115	H
A_2 ($\times 10^{-4}$)	0.297	0.291	0.221	0.182	0.153	m^2
A_{C2} ($\times 10^{-6}$)	0.684	0.669	0.592	0.535	0.493	m^2
Z_2 ($\times 10^{-1}$)	0.405	0.396	0.356	0.329	0.311	m
L_2 ($\times 10^{-4}$)	0.899	0.854	0.598	0.469	0.384	H
A_6 ($\times 10^{-4}$)	0.675	0.639	0.602	0.557	0.518	m^2
A_{C6} ($\times 10^{-6}$)	0.738	0.725	0.681	0.647	0.616	m^2
Z_6 ($\times 10^{-1}$)	0.452	0.438	0.422	0.409	0.399	m
L_6 ($\times 10^{-4}$)	0.929	0.919	0.880	0.831	0.781	H
C_3 ($\times 10^{-3}$)	0.100	0.948	0.897	0.823	0.758	F
C_4 ($\times 10^{-4}$)	0.155	0.142	0.0485	0.0477	0.0466	F
C_5 ($\times 10^{-3}$)	0.307	0.205	0.157	0.127	0.107	F

Table (4.4-2)

Component Design Values of Cuk Converter as a Function of Frequency

	20 KHZ	30 KHZ	40 KHZ	50 KHZ	60 KHZ	Unit
A_1 ($\times 10^{-4}$)	0.468	0.467	0.295	0.235	0.211	m^2
A_{C1} ($\times 10^{-6}$)	0.632	0.624	0.467	0.389	0.341	m^2
Z_1 ($\times 10^{-1}$)	0.440	0.438	0.376	0.331	0.305	m
L_1 ($\times 10^{-3}$)	0.179	0.178	0.116	0.085	0.075	H
A_2 ($\times 10^{-4}$)	0.347	0.302	0.244	0.197	0.183	m^2
A_{C2} ($\times 10^{-6}$)	0.743	0.715	0.599	0.519	0.474	m^2
Z_2 ($\times 10^{-1}$)	0.427	0.408	0.349	0.316	0.307	m
L_2 ($\times 10^{-4}$)	0.598	0.597	0.388	0.285	0.252	H
A_6 ($\times 10^{-4}$)	0.177	0.152	0.122	0.110	0.101	m^2
A_{C6} ($\times 10^{-6}$)	0.217	0.208	0.173	0.154	0.124	m^2
Z_6 ($\times 10^{-1}$)	0.307	0.294	0.263	0.247	0.223	m
L_6 ($\times 10^{-3}$)	0.103	0.102	0.834	0.787	0.762	H
C_3 ($\times 10^{-3}$)	0.851	0.848	0.676	0.575	0.491	F
C_4 ($\times 10^{-3}$)	0.111	0.100	0.028	0.027	0.022	F
C_5 ($\times 10^{-3}$)	1.130	0.526	0.410	0.309	0.248	F

2. Source weight

3. Packaging and heat sink weight

(b) Quantities that decrease with frequency:

1. Core weight

2. Winding weight

3. Capacitor weight

(3) Profiles of Magnetic and Capacitive Sizes

Quantities that decrease with switching frequency are shown in the following:

1. Core cross-section area

2. Core mean magnetic path length

3. Wire size

4. Capacitance

5. Inductance

The benefit of operating the switching power converter at high frequency end is supported by the fact that the magnetic and capacitive components decrease all the way with the increasing switching frequency, unfortunately the increasing device switching losses and magnetic losses with increasing switching frequency sets the limit of the maximum operating frequency for the optimum design.

CHAPTER 5

DESIGN-ORIENTED SENSITIVITY ANALYSIS

In this chapter, the effects of using different input voltages and different core materials with different saturation flux densities on the total power converter optimization are presented. This sensitivity analysis by perturbing the operating point can provide valuable design insights into the power converter global optimization problem. Usually before the optimization task is taken, the performance requirements and the design constants are specified. Three parameters are of particular interest in the role of the optimization of the switching power converter, that is, the transistor switching speed, the input voltage, and the use of different core materials with different saturation flux densities. The effect of the transistor switching speed on the power converter optimization has already been investigated in the author's publication (61). The effect of the other two factors are investigated in the following by taking the Cuk converter as a demonstration example. The analysis can also be applied to other types of switching power converters.

5.1 Effect of Input Voltage

Usually in a power converter design optimization, the output voltage level is specified along with the required ripple factor performance. Depending on the system voltage source limitations, the input voltage may be available over a wide range. Since the input

voltage is related to the average input current and since the average input current is related to the power loss of the components through which the current passes, the choice of the input voltage plays an important role in the overall system performance. The Cuk converter is taken as an example to study the effect of different input voltages on the total power converter performance.

The loss and weight breakdowns with input voltages of 10V, 15V, and 42V are tabulated in Table (5.1-1). These results were obtained by the NLP optimization algorithm described earlier. Examination of this table reveals some significant differences in the overall power converter performance with different input voltages. Therefore, if the input voltage is not specifically specified in a power converter optimization, it must be considered as an important factor in determining the global system optimization.

Discussion:

(1) Examination of Table (5.1-1) reveals that the input filter magnetic losses PIF decrease with increasing input voltage rapidly, while at the same time, the output filter magnetic losses (POF) increase only moderately. Due to the decreasing average input current and the increasing output current, the magnetic losses are steered from the input port to the output port with the input filter magnetic losses decreasing more rapidly, thus resulting in a decreasing total magnetic loss shown as PMAG in the table. The decreasing magnetic losses account for the decreasing total losses with the increasing input voltage. With the

Table (5.1-1)

Comparison of Loss and Weight Breakdowns of the Cuk Converter with Input Voltages at 10V, 15V, and 42V Respectively and and Output Voltage Fixed at 28V

	Input Voltage	10V	15V	42V
	F(HZ)	39,238	39,276	61,666
Loss (Watts):	PIF	5.479	2.130	0.424
	PQ	3.166	2.172	1.609
	PD	2.357	2.174	2.062
	PERS	0.272	0.0483	0.0482
	POF	0.935	1.034	2.131
	PMAG	6.414	3.164	2.554
	PT	11.965	7.559	6.273
Weight (kg):	WI	0.0205	0.0176	0.0087
	WW	0.0179	0.0161	0.0084
	WIW	0.0384	0.0337	0.0171
	WS	2.3356	2.1919	2.1502
	WH	0.7752	0.4878	0.4042
	WC	0.0203	0.0207	0.0081
	WMAG	0.6632	0.3418	0.2658
	W	3.1695	2.7341	2.5796

output voltage still set at 28 volts, it is recommended that better efficiency can be obtained by operating the power converter in the step-down mode. It is also interesting to note that the decrease of the total loss from 10 volts to 15 volts is much larger than the decrease from 15 volts to 42. This fact points out that the decrease of the total losses, with higher input voltages, reaches a saturation point as the input voltage increases beyond certain levels.

(2) By examining the weight breakdowns, it is noticed that the total system weight is decreasing with increasing input voltage. The weight decrease is due to the decreasing source and heat sink weights caused by the decreasing magnetic total losses discussed previously. Again a diminishing return of weight savings as the input voltage increases beyond a certain point is also noticed.

5.2 Effect of Maximum Operating Flux Density

Since the magnetic components constitute one of the major ingredients of the switching power converter, it is significant to study the effect of using different core materials on the total power converter performance. It is well known that different core materials have different maximum operating flux densities before saturation is reached. For example, the Permalloy (79% nickel - 17% iron) and the Orthonol (50% nickel - 50% iron) have the maximum flux densities around 0.4 Weber/m^2 and 1.2 Weber/m^2 respectively. Again the Cuk converter is taken as an example to study the effect of different core materials on the total power converter performance. The loss and weight

breakdowns obtained through the nonlinear programming for core materials with maximum flux densities of 0.4, 0.8, and 1.2 Webers/m^2 are given in Table (5.2-1). There are significant weight savings by using higher flux density core material. Thus, the selection of core material must be considered in determining the global system optimization.

Discussion:

(1) The decreasing magnetic core size by using higher flux density core results in a decreasing magnetic core weight and winding weight shown as WIW in the Table.

(2) The decreasing total magnetic losses by using higher flux density cores accounts for the majority of the reduction in the total losses. This also results in a reduction of source and heat sink weights.

(3) Again the diminishing return of loss and weight reduction with the increasing core flux density is observed for the total loss and total weight.

Table (5.2-1)

Comparison of Loss and Weight Breakdowns of Cuk Converter with the Maximum Operating Flux Densities of 0.4, 0.8 and 1.0 Weber/m^2

Flux Density		0.4	0.8	1.2
	F(HZ)	39,276	39,276	39,276
Loss (Watts):	PIF	2.1299	1.4564	1.2192
	PQ	2.1722	2.1259	2.1164
	PD	2.1745	2.1793	2.1736
	PERS	0.0483	0.0417	0.0384
	POF	1.0338	0.6965	0.6023
	PMAG	3.1637	2.1529	1.8215
	PT	7.5588	6.4998	6.1499
Weight (kg):	WIW	0.0337	0.0326	0.0233
	WS	2.1919	2.1591	2.1477
	WH	0.4878	0.4221	0.3993
	WC	0.0207	0.0167	0.0149
	WMAG	0.3418	0.2423	0.2007
	W	2.7341	2.6304	2.5853

CHAPTER 6

CONCLUSIONS AND RECOMMENDATIONS

A nonlinear programming technique using the penalty function method has been presented and utilized for the comparison of the conventional Buck-Boost and Cuk converters. Detailed comparisons were made with respect to the loss and weight breakdowns. The comparison showed that the Cuk converter outperforms the conventional Buck-Boost converter in both operating efficiency and weight considerations for both step up and step down modes of operation.

The practical programming aspects for utilizing the variable and constraint scaling techniques to speed up the rate of convergence were elaborated upon and an efficient programming approach was proposed for a successful implementation. The importance of a carefully chosen initial starting point on the speed of convergence was also discussed.

In addition to the detailed comparison of loss and weight breakdowns of the Cuk and Buck-Boost converters, a comparison of the coupled-inductor Cuk converter for the balanced and unbalanced current ripple reduction modes was made and it was concluded that the unbalanced condition was more advantageous.

The global optimization aspect was investigated through the design oriented sensitivity analysis by perturbing two of the most important parameters. Significant differences were observed by

perturbing the input voltage and the maximum operating flux density. This study sheds some light on the global system optimization.

The application of the nonlinear programming technique to the power converter design optimization through the availability of the high speed digital computer not only facilitated the comparisons but also proved to be cost-effective in the power converter design optimization. The conventional approach using the iterative process could thus be abandoned.

Future extensions of this work should include an investigation of the utilization of the power MOSFET instead of the power transistor. With the introduction of the high power, high speed power MOSFET's it is now possible to operate the switching power converters to the Megahertz range for the first time, thus further reducing the size and weight to take full advantage of the benefits of operating at very high frequencies (62-66). One of the most important contributions is the size reduction of the EMI filter. However, the benefits of operating at very high frequency range are not without penalty. The design of high frequency magnetics becomes more difficult and complicated considering that the magnetic skin effect becomes very pronounced above 100 KHZ. The modeling of the magnetic core and copper losses thus become much more difficult and a good model is needed for the computer simulation of the loss profiles. More work needs to be done in this area.

Finally, the contributions of this work are stated briefly in the following:

(1) For the first time nonlinear programming techniques were used to

evaluate and compare the performance of the optimum designs of the Cuk and conventional Buck-Boost converters. The evaluation and comparison were based on:

(a) The same number of components

(b) The same EMI filter requirements

(c) The same power output

(d) The same input and output voltages

(e) The same output voltage ripple factor

(f) The same core material and core configuration

(g) The same number of design constraints

The following performance indices were also compared extensively:

(a) Detailed loss breakdowns

(b) Detailed weight breakdowns

(c) Percentage contributions of loss and weight breakdowns

(2) For the first time the nonlinear programming techniques were used to study the coupled inductor version of the Cuk converter for both the balanced and unbalanced current ripple reduction. Detailed comparisons were made of the loss and weight breakdowns.

(3) For the first time the nonlinear programming was used to perform the sensitivity analysis of the switching power converter. This analysis provides valuable information on the global optimization of the power converter design.

Finally, the comparison and evaluation of the optimum Cuk and conventional Buck-Boost converters revealed that the Cuk converter is superior to the conventional Buck-Boost converter in both the step up and step down modes of operation.

LIST OF REFERENCES

1. Pressman, Abraham I., "Switching and Linear Power Supply, Power Converter Design," Hayden Book Co., Inc., 1977, Chapter 6.

2. Holt, Charles A., "Electronic Circuits, Digital and Analog," John Wiley & Sons, Inc., 1978, Chapter 24.

3. Patchett, G. N., "Electronic Power Supplies," Pitman Publishing, 1970.

4. Traister, Robert J., "DC Power Supplies, Application and Theory," Reston Publishing Co., Inc., 1979.

5. Feng, S. Y., Wilson, T. G., and Sander, W. A., "Very High Frequency DC-to-DC Conversion and Regulation in the Low Megahertz Range," IEEE Power Electronics Specialists Conference, 1971 Record, pp. 58-65.

6. Sevens, R. P., "High Frequency Switching Regulator Techniques," IEEE Electronics Specialists Conference, 1978 Record, pp. 290-298.

7. Sevens, R. P., "The Design of Switchmode Converters Above 100 KHZ," Intersil, Inc., Application Bulletin A034.

8. Sevens, R. P., "The Design of High Efficiency Off-Line Converters Above 100 KHZ," Powercon 5 Conference Record, May 1978.

9. Sloane, T. H., Owen, H. A., Jr., and Wilson, T. G., "Switching Transients in High-Frequency High-Power Converters Using Power MOSFET's," IEEE Power Electronics Specialists Conference, 1979 Record, pp. 244-254.

10. Bahler, David D., Owen, H. A., Jr., and Wilson, T. G., "Predicting Performance of Power Converters Operating with Switching Frequencies in the Vicinity of 100 KHZ," IEEE Power Electronics Specialists Conference, 1978 Record, pp. 148-157.

11. Landsman, E. E., "A Unifying Derivation of Switching DC-DC Converter Topologies," IEEE Power Electronics Specialists Conference, 1979 Record, pp. 239-243.

12. Wood, Peter, "General Theory of Switching Power Converters," IEEE Power Electronics Specialists Conference, 1979 Record, pp. 3-10.

13. Cuk, Slobodan and Middlebrook, R. D., "A New Optimum Topology Switching DC-to-DC Converter," IEEE Power Electronics Specialists Conference, 1977 Record, pp. 160-179.

14. Cuk, Slobodan and Middlebrook, "Coupled-Inductor and Other Extensions of a New Optimum Topology Switching DC-to-DC Converter," IEEE Industry Applications Society Annual Meeting, 1977 Record, pp. 1110-1126.

15. Middlebrook, R. D. and Cuk, Slobodan, "Isolation and Multiple Output Extensions of a New Optimum Topology Switching DC-to-DC Converter," IEEE Power Electronics Specialists Conference, 1978 Record, pp. 256-264.

16. Middlebrook, R. D., Cuk, Slobodan, and Behen, W., "A New Battery Charger/Discharger Converter," IEEE Power Electronics Specialists Conference, 1978 Record, pp. 251-255.

17. Cuk, Slobodan and Erickson, Robert W., "A Conceptually New High-Frequency Switched-Mode Amplifier Technique Eliminates Current Ripple," Proc. Fifth National Solid-State Power Conversion Conference (Powercon 5), pp. G3.1-G3.22, May 1978.

18. Cuk, Slobodan, "General Topological Properties of Switching Structures," IEEE Power Electronics Specialists Conference, 1979 Record, pp. 109-130.

19. Cuk, Slobodan, "Switching DC-to-DC Converter with Zero Input or Output Current Ripple," IEEE Industry Application Society Annual Meeting, 1978 Record, pp. 1131-1146.

20. Cuk, Slobodan, "A New Zero-Ripple Switching DC-to-DC Converter and Integrated Magnetics," IEEE Power Electronics Specialists Conference, 1980 Record, pp. 12-32.

21. Middlebrook, R. D. and Cuk, S., "A General Unified Approach to Modeling Switching-Converter Power Stages," IEEE Power Electronics Specialists Conference, 1976 Record, pp. 18-34.

22. Middlebrook, R. D. and Cuk, S., "Modeling and Analysis Methods for DC-to-DC Switching Converters," IEEE International Semiconductor Power Converter Conference, 1977 Record, pp. 90-111.

23. Wu, C. J., Lee, F. C., Balachandran, S., and Goin, H. L., "Design Optimization for Half-Bridge DC-DC Converter," IEEE Power Electronics Specialists Conference, 1980 Record, pp. 57-67.

24. Moore, E. T. and Wilson, T. G., "Basic Considerations for DC to DC Conversion Network," IEEE Trans. on Magnetics, Vol. MAG-2, No. 3, Sept. 1966, pp. 620-624.

25. Kossov, O. A., "Comparative Analysis of Chopper Voltage Regulations with LC Filter," IEEE Trans. on Magnetics, Vol. MAG-4, No. 4, December 1968, pp. 712-715.

26. Hoo, S. K., "On Some General Laws of DC-DC Regulators," IEEE 1972 Intermag Conference, Sept. 1972, pp. 291-293.

27. Wester, G. W., "Low-Frequency Characterization of Switched DC-DC Converters, Ph.D. Thesis, California Institute of Technology, Pasadena, May 1972.

28. Wester, G. W. and Middlebrook, R. D., "Low-Frequency Characterization of Switched DC-DC Converters," IEEE Trans. Aerospace and Electronic Systems, Vol. AES-9, May 1973, pp. 376-385.

29. Ogata, K., "Modern Control Engineering," Prentice-Hall Inc., 1970 Edition, Chapter 11.

30. Middlebrook, R. D., "Describing Function Properties of a Magnetic Pulse-Width Modulator," IEEE Power Electronics Specialists Conference, 1972 Record, pp. 21-35.

31. Middlebrook, R. D., "Describing Function Properties of a Magnetic Pulse-Width Modulator," IEEE Trans. on Aerospace and Electronic Systems, Vol. AES-9, No. 3, May 1973, pp. 386-398.

32. Wester, G. W., "Stability Analysis and Compensation of a Boost Regulator with Two-Loop Control," IEEE Power Electronics Specialists Conference, 1974 Record, pp. 237-245.

33. Wester, G. W., "Linearized Stability Analysis and Design of a Flyback DC-DC Boost Regulator," IEEE Power Electronics Specialists Conference, 1973 Record, pp. 130-137.

34. Capel, A., Ferrante, J. G., and Prajoux, R., "Stability Analysis of a P.W.M. Controlled DC/DC Regulator with DC and AC Feedback Loops," IEEE Power Electronics Specialists Conference, 1974 Record, pp. 246-254.

35. Capel, A., Ferrante, J. G., and Prajoux, R., "State Variable Stability Analysis of Multi-Loop PWM Controlled DC/DC Regulators in Light and Heavy Mode," IEEE Power Electronics Specialists Conference, 1975 Record, pp. 91-103.

36. Yu, Yuan and Biess, J. J., "Some Design Aspects Concerning Input Filters for DC-DC Converters," IEEE Power Electronics Specialists Conference, 1971 Record, pp. 66-76.

37. Sokal, N. O., "System Oscillations Caused by Negative Input Resistance at the Power Input Port of a Switching Mode Regulator, Amplifier, DC/DC Converter, or DC/AC Inverter," IEEE Power Electronics Specialists Conference, 1973 Record, pp. 138-140.

38. Middlebrook, R. D., "Input Filter Considerations in Design and Applications of Switching Regulators," IEEE Industry Applications Society Annual Meeting, 1976 Record, pp. 366-382.

39. Middlebrook, R. D., "Design Techniques for Preventing Input-Filter Oscillations in Switched-Mode Regulators," Proc. Fifth National Solid-State Power Conversion Conference (Powercon 5). pp. A3-1-A3-16.

40. Matsuo, H. and Harada, K., "The Cascaded Connection of Switching Regulators," IEEE Trans. on Industry Applications, Vol. IA-3, No. 2, Mar./Apr. 1976.

41. Harada, K. and Matsuo, H., "A Method of Surge Reduction in the Switching Regulator," IEEE Power Electronics Specialists Conference, 1976 Record, pp. 303-311.

42. Wilson, T. G., Jr., "Cross Regulation in an Energy-Storage DC-to-DC Converter with Two Regulated Outputs," IEEE Power Electronics Specialists Conference, 1977 Record, pp. 190-199.

43. Wilson, T. G., Jr., "Cross Regulation in a Two-Output DC-to-DC Converter with Application to Testing of Energy-Storage Transformers," IEEE Power Electronics Specialists Conference, 1978 Record, pp. 124-134.

44. Owen, H. A., Jr., Wilson, T. G., Jr., Feng, Y. M. and Lee, C. Y., "A Computer-Aided Design Procedure for Flyback Step-Up DC-to-DC Converters," IEEE Trans. on Magnetics, Vol. MAG-8, pp. 289-291, Sept. 1972.

45. Chen, D. Y., Owen, H. A., Jr., and Wilson, T. G., Jr., "Table-Aided Design of the Energy-Storage Reactor in DC-to-DC Converters," IEEE Trans. on Aerospace and Electronic Systems, Vol. AES-12, No. 3, May 1976, pp. 374-386.

46. Chen, D. Y., Owen, H. A., Jr., and Wilson, T. G., Jr., "Energy-Balance Constraints Affecting the Design of Energy-Storage DC-to-DC Converters," 1975 IEEE Applied Magnetics Workshop, June 1975, Milwaukee, WI.

47. Judd, F. F. and Kressler, D. R., "Design Optimization of Small Low-Frequency Power Transformers," IEEE Trans. on Magnetics, Vol. MAG-13, No. 4, July 1977.

48. Yu, Yuan, Bachmann, Max, and Lee, C. Y., "Formulation of a Methodology for Power Circuit Design Optimization," IEEE Power Electronics Specialists Conference, 1976 Record, pp. 35-44.

49. Ingram, D. L., "Designing Switched-Mode Converter Systems for Compliance with FCC Proposed EMI Requirement," Proc. Fourth National Solid-State Power Conversion Conference (POWERCON 4), pp. G1-1 to G1-11, 1977.

50. Bloom, S. D. and Massey, R. P., "Emission Standards and Design Techniques for EMI Control of Multiple DC-DC Converter Systems," IEEE Power Electronics Specialists Conference, 1976 Record, pp. 312-317.

51. Rhoades, W. T. and Levine, L., "Conducted EME Design Techniques for Commercial Multinational Switching Power Supplies," Proc. Fifth National Solid-State Power Conversion Conference (POWERCON 5) pp. H2-1 to H2-9, May 1978.

52. Skanadore, W. R., "Reducing Conducted EMI with a New Ultra-Low-Capacitance Switching Transistor Configuration," Proc. Fifth National Solid-State Power Conversion Conference (POWERCON 5), pp. H4-1 to H4-10, May 1978.

53. Burens, James H., "Specifying and Measuring Switching Power Supply Parameters," Proc. Fourth National Solid-State Power Conversion Conference (POWERCON 4), pp. F2-1) to F2-10), 1977.

54. Loftis, C. B., "Optimizing Dynamic Characteritistics of High Voltage Switched Mode Converters," Solid State Power Conversion, July/August 1978, pp. 50-59.

55. Courant, R., "Variational Methods for the Solution of Problems of Equilibrium and Variations," Bulletin of the American Math Society, Vol. 49, pp. 1-23, Jan. 1943.

56. Carroll, C. W., "The Created-Response-Surface Technique for Optimizing Nonlinear Restrained Systems," Operations Research, Vol. 9, pp. 169-184, March/April 1961.

57. Fiacco, A. V. and McCormick, G. P., Nonlinear Programming: Sequential Unconstrained Minimization Techniques, Book by Wiley, New York, 1968.

58. Fletcher, R., "A Class of Methods for Nonlinear Programming with Termination and Convergence Properties," Chapter 6 of Integer and Nonlinear Programming, J. Abadie (Editor), North-Holland Publishing Co., Amsterdam, 1970.

59. Fletcher, R., "Methods Related to Lagrangian Functions," in Numerical Methods for Constrained Optimization, Academic Press, 1974, pp. 219-240.

60. Pierre, D. A. and Lowe, M. J., Mathematical Programming Via Augmented Lagrangians, An Introduction with Computer Programs, Book By Addison - Wesley Publishing Co., Inc., 1975.

61. Wu, C. J., Lee, F. C., and Balachandran, S., "Design Optimization for a Half-Bridge DC-DC Converter," IEEE Power Electronics Specialists Conference, 1980 Record, pp. 57-67.

62. Severns, Rudy, "The Design of Switchmode Converters Above 100 KHZ," Intersil Application Bulletin A034.

63. Shaeffer, Lee, "Improving Converter Performance and Operating Frequency with a New Power FET," Proc. Fourth National Solid-State Power Conversion Conference (POWERCON 4), pp. C2-1 to C2-8)

64. Severns, Rudolf P., "High Frequency Switching Regulator Techniques," IEEE Power Electronics Specialists Conference, 1978 Record, pp. 290-298.

65. Severns, Rudy, "The Power MOSFET, A Breakthrough in Power Device Technology," Intersil Application Bulletin A033.

66. Bahler, D. A., Owen, H. A., Jr., and Wilson, T. G., Jr., "Predicting Performance of Power Converters Operating with Switching Frequencies in the Vicinity of 100 KHZ," IEEE Power Electronics Specialists Conference, 1978 Record, pp. 148-157.

The vita has been removed from the scanned document

ANALYSIS, DESIGN, AND EVALUATION OF THE OPTIMUM TOPOLOGY CUK CONVERTER IN COMPARISON WITH THE CONVENTIONAL BUCK-BOOST CONVERTER

by

Ching Jang Wu

(ABSTRACT)

A nonlinear programming technique using the penalty function method,which is especially suitable for power converter design optimization, is utilized for the comparison of the conventional Buck-Boost and Cuk converters. Detailed comparisons are made with respect to the loss and weight breakdowns of the optimum design of the two converters for a given set of performance specifications. The comparison shows that the Cuk converter outperforms the conventional Buck-Boost converter in both operating efficiency and weight considerations for both the step up or step down modes of operation. Also, a detailed comparison of the coupled inductor version of the Cuk converter under both the balanced and unbalanced current ripple reduction modes of operation is made. From this comparison, it is shown that the unbalanced current ripple reduction is more advantageous. The effects of using different input voltages and different core materials with different saturation flux densities on the global power converter optimization were also studied.

The new Cuk converter was disclosed for the first time in 1977. Since then, there are several controversies about the claims made by Cuk of the advantages of his converter with respect to the conventional Buck-Boost converter. The comparisons made by Cuk of the

two converters did not satisfy the same performance specifications. Consequently, his conclusions of the superiority of his converter cannot be fully justified. In this work, the comparisons are made of these two converters based upon the optimum designs for a given set of performance specifications. With the detailed comparisons of the loss/weight breakdowns of these two converters, the controversies surrounding the Cuk converter are solved.